Biomaterials 183 (2018) 185–199

Contents lists available at ScienceDirect

Biomaterials

journal homepage: www.elsevier.com/locate/biomaterials

Antibacterial adhesive injectable hydrogels with rapid self-healing, extensibility and compressibility as wound dressing for joints skin wound healing

Jin Qu[a,1], Xin Zhao[a,1], Yongping Liang[a], Tianlong Zhang[a], Peter X. Ma[b,c,d,e], Baolin Guo[a,*]

[a] Frontier Institute of Science and Technology, And State Key Laboratory for Mechanical Behavior of Materials, Xi'an Jiaotong University, Xi'an, 710049, China
[b] Department of Biomedical Engineering, University of Michigan, Ann Arbor, MI 48109, USA
[c] Department of Biologic and Materials Sciences, University of Michigan, Ann Arbor, MI 48109, USA
[d] Macromolecular Science and Engineering Center, University of Michigan, Ann Arbor, MI 48109, USA
[e] Department of Materials Science and Engineering, University of Michigan, Ann Arbor, MI 48109, USA

ARTICLE INFO

Keywords:
Wound dressing
Injectable self-healing hydrogel
Antibacterial activity
Curcumin
Hemostat
Adhesive

ABSTRACT

Designing wound dressing materials with outstanding therapeutic effects, self-healing, adhesiveness and suitable mechanical property has great practical significance in healthcare, especially for joints skin wound healing. Here, we designed a kind of self-healing injectable micelle/hydrogel composites with multi-functions as wound dressing for joint skin damage. By combining the dynamic Schiff base and copolymer micelle cross-linking in one system, a series of hydrogels were prepared by mixing quaternized chitosan (QCS) and benzaldehyde-terminated Pluronic®F127 (PF127-CHO) under physiological conditions. The inherent antibacterial property, pH-dependent biodegradation and release behavior were investigated to confirm multi-functions of wound dressing. The hydrogel dressings showed suitable stretchable and compressive property, comparable modulus with human skin, good adhesiveness and fast self-healing ability to bear deformation. The hydrogels exhibited efficient hemostatic performance and biocompatibility. Moreover, the curcumin loaded hydrogel showed good antioxidant ability and pH responsive release profiles. *In vivo* experiments indicated that curcumin loaded hydrogels significantly accelerated wound healing rate with higher granulation tissue thickness and collagen disposition and upregulated vascular endothelial growth factor (VEGF) in a full-thickness skin defect model. Taken together, the antibacterial adhesive hydrogels with self-healing and good mechanical property offer significant promise as dressing materials for joints skin wound healing.

1. Introduction

Skin damage is one of the most common physical injury throughout human history [1,2]. Designing new wound dressing materials has been an imperative issue in modern medical technology finding [3,4]. Among these novel dressing materials fabricated in recent years, hydrogel with high-water content and biocompatibility is considered as a promising candidate for practical application [1,5,6]. Firstly, by providing a porous structure and suitable swelling ratio, hydrogel matrix can allow for oxygen presence, absorb the exudates, maintain moist healing environment [7] to promote wound healing [8]. Secondly, hydrogel adhesives could isolate the external bacteria cloning and promote gaseous exchange that inhibits the proliferation of anaerobic bacteria [9–12]. Furthermore, the antibacterial property of traditional dressing is endowed by antibiotics capsulated in the hydrogel matrix [13]. However, the dressing material with inherent antimicrobial property is more attractive, because this kind of inherent antibacterial hydrogel could present consistent antibacterial activity [14–17]. Thirdly, unlike traditional wound dressing (gauze and cotton wool), bioactive molecules loaded hydrogel dressings exhibited desirable biological activity by releasing encapsulated drug from the hydrogel matrix. The released drug molecules play an imperative role on wound healing [5,14], such as curcumin which has powerful modulating effects on every phase of wound healing [18–20]. Fourthly, physiological milieu of the wounded skin is faintly acidic [21]. Thus, pH-responsive hydrogel dressing which could release encapsulated drug smartly was more beneficial to the actual needs.

In addition, traditional dressing material such as bandage faces

* Corresponding author.
E-mail address: baoling@mail.xjtu.edu.cn (B. Guo).
[1] These authors contributed equally to this work.

https://doi.org/10.1016/j.biomaterials.2018.08.044
Received 3 July 2018; Received in revised form 12 August 2018; Accepted 20 August 2018
Available online 24 August 2018
0142-9612/

considerable problems in joint wound [22]. Bruises and scrapes on extremities make up majority of skin trauma. Due to the frequent motion and bending, like ankle, knee and wrist, when the traditional dressing materials are applied on these joints, patients are tied with them, which dramatically increases their discomfort and inconvenience. The unstable connection between dressing materials and wound site also weakens their availability and reliability [23]. On the contrary, hydrogel with moderate stretching and compressive capacity, good interfacial adhesion and comparable modulus with human soft tissue [24,25] renders us a brand-new choice as wound dressing for joints. This kind of hydrogel can tolerate mechanical deformation caused by movements of the extremities and thus provide stable connection between joint and dressing material. Furthermore, accidental external mechanical force may cause avulsion of dressing materials [24,26,27]. While hydrogel dressing with rapid self-healing ability could repair the damage automatically and prolong the service time [28–31]. Single dynamic covalent bonds (Schiff base) were employed to re-establish hydrogel networks to get their desirable self-healing property in our prior work [1,16,32]. While in the recent work, the hydrogel integrating two or more kinds of physical and chemical interactions in one system endows the material more stable mechanical properties and excellent self-healing ability [12,33–36], which is attributed to the combined action between effective energy dissipation mechanism and the effect of dynamic chemical covalent bonds [37,38]. Upon loading or deformation, physical interactions could dissipate energy, and these interactions can reform during unloading or resting, leading to the recovery of this kind of hybrid hydrogel composites from damages and fatigues [39]. While, combination of malleability, compressibility, fatigue resistance properties, and self-healing ability in one hydrogel system as wound dressing is highly challenging. Due to these superior abilities, this kind of self-healing hydrogel is capable of sealing the wound site completely on the precondition of patients' practical need and protect it from a second injury [1]. Until now, as a kind of novel wound dressing, especially for joint skin wound care, the injectable hydrogel which integrates multi-functions, including inherent antibacterial activity, adhesiveness, hemostasis, pH responsiveness, desirable mechanical property and self-healing ability, has not been reported.

This work reports a series of versatile injectable hydrogels with self-healing, adhesiveness, stretchability, hemostasis, pH responsiveness and inherent antibacterial property as novel joint skin wound dressing. We furthermore demonstrated that these hydrogel dressings greatly promoted the healing process compared to commercial dressing (Tegaderm™) in a full-thickness skin defect model. The hydrogels were prepared by mixing quaternized chitosan (QCS) solution and benzaldehyde-terminated poly(ethylene oxide)-*b*-poly(propylene oxide)-*b*-poly(ethylene oxide) (PEO_{99}-*b*-PPO_{65}-*b*-PEO_{99}, Pluronic® F127 (PF127)) (PF127-CHO) solution at different -CHO/-NH_2 ratios under physiological conditions (Fig. 1a and b). PF127 was chosen as a crosslinker due to its good property of self-assembly into micelle in water and good biocompatibility [40–42]. In this work, we combined the dynamic Schiff base bond and PF127 micelle cross-linking as two kinds of dynamic crosslinking in one hydrogel to get excellent mechanical property and self-healing ability (Fig. 1c). The hydrogel exhibited excellent malleability and compressible property and self-healing ability under multi-cyclic deformation. And these series of hydrogels exhibited excellent antibacterial property, biocompatibility, efficient blood clotting capacity, and good adhesiveness compared to the previous reported injectable hydrogels. [43–46] In addition, the curcumin loaded hydrogel (Cur-QCS/PF) showed tunable antioxidant ability. Furthermore, the results of wound contraction area, histopathological examinations, biochemical analysis and immunofluorescence staining were employed to evaluate the *in vivo* therapeutic effects of Cur-QCS/PF hydrogel dressing. All the data indicated that these antibacterial adhesive injectable self-healing hydrogels with excellent mechanical properties show great potential as wound dressing especially for joints skin wound healing.

2. Experimental section

2.1. Materials

Chitosan (M_n = 100000–300000 Da) was obtained from J&K Scientific Ltd. Glycidyltrimethylammonium chloride (GTMAC), poly (ethylene oxide)-*b*-poly(propylene oxide)-*b*-poly(ethylene oxide) (PEO_{99}-*b*-PPO_{65}-*b*-PEO_{99}, Pluronic® F127 (PF127)), 4-hydroxybenzaldehyde, and curcumin were purchase from Sigma. All other reagents were used without further purification.

2.2. Synthesis of quaternized chitosan (QCS)

QCS was synthesized according to our previous publications with some modifications [1,47]. The details are available in SI Materials and methods.

2.3. Synthesis of benzaldehyde-terminated PF127 (PF127-CHO)

PF127-CHO was synthesized by using a procedure with some modifications [33,35]. The details are available in SI Materials and methods. The structure of PF127-CHO was confirmed by ^{1}H NMR spectra as shown in Fig. S1.

2.4. Preparation of curcumin loaded PF127-CHO micelles (Cur-PF127-CHO)

Cur-PF127-CHO micelles were synthesized by a one-step solid dispersion method [5,48]. The Cur-PF127-CHO solution was stored at 4 °C before use. The details are available in SI Materials and methods.

2.5. Synthesis of QCS/PF and Cur-QCS/PF hydrogels

QCS polymer was dissolved in phosphate-buffered saline (PBS) to form 5% *wt/vol* QCS solution at 55 °C. To tune molar ratio (R = 0.8–1.3) of -CHO/-NH_2, the desired amount of PF127-CHO was dissolved in PBS (pH = 7.4) to form 24–40% (*wt/vol*) solutions. The hydrogels were prepared by mixing QCS solution and PF127-CHO solution in a ratio of 2:3 (*v/v*) at 37 °C, and the hydrogel samples were shown in Fig. 2a. The method of recording the gelation time is tube inversion method [49]. After the dissolution of PF127-CHO and QCS polymer in a centrifuge tube, the sol-to-gel transition of QCS and PF127-CHO mixture at 37 °C was determined by tube inversion every 10 s. When the hydrogel precursor stopped flowing upon tube inversion, the gelation time was recorded.

For Cur-QCS/PF hydrogels, they were prepared with a similar way of QCS/PF hydrogels, except that using Cur-PF127-CHO solutions as crosslinker.

2.6. Characterization

The fourier transform infrared spectroscopy (FT-IR), the ^{1}H nuclear magnetic resonance (^{1}H NMR), thermogravimetric analysis (TGA), dynamic light scattering (DLS), scanning electron microscope (SEM), transmission electron microscope (TEM), injectability, rheological properties, swelling ratio, *in vitro* degradation and water vapor permeability [50–52] were used to investigate the chemical and physical characterizations of copolymer samples or hydrogels. The details are available in SI Materials and methods.

2.7. Self-healing performance of hydrogels

Macroscopic self-healing experiments and quantitative self-healing test were chosen to evaluate the self-healing performance of hydrogels

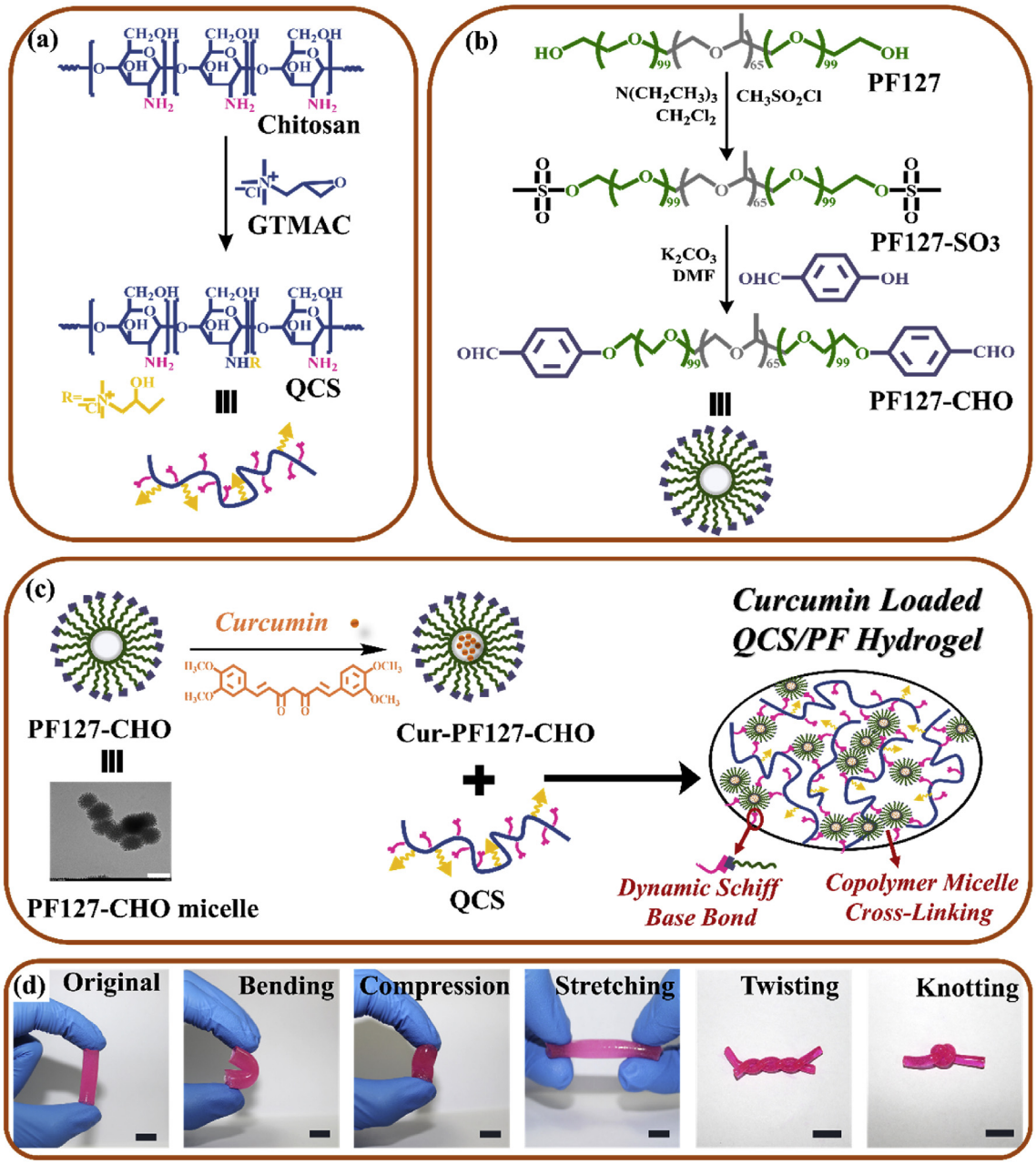

Fig. 1. Schematic representation of Cur-QCS/PF hydrogel synthesis. (a) Synthesis scheme of QCS polymer, (b) PF127-CHO polymer, (c) Schematic illustration of Cur-QCS/PF hydrogel and TEM image of PF127-CHO micelles. Scale bar: 200 nm. (d) The original, bending, compression, stretching, twisting and knotting shapes of rhodamine B dyed QCS/PF1.0 hydrogels. Scale bar: 1 cm.

[32]. The details are available in SI Materials and methods.

2.8. In vitro drug release study

Different pH values of PBS (pH value = 7.4, 6.8, 6.0) were chosen to evaluate the *in vitro* drug release behavior of hydrogels and the released behavior of hydrogels from different crosslinking density (Cur-QCS/PF1.3, Cur-QCS/PF1.2, Cur-QCS/PF1.0, Cur-QCS/PF0.8) was tested [53]. The details are available in SI Materials and methods.

2.9. Mechanical properties of QCS/PF hydrogel

The mechanical tensile stress−strain tests were evaluated by the uniaxial tensile test employing an Instron materials test system (MTS Criterion 43; MTS Criterion) equipped with a 50 N tension sensor [54–56]. The compressive and recovery properties were investigated using a rheometer (Model DHR-2, TA Instruments). The details are available in SI Materials and methods.

2.10. Adhesive strength test of the hydrogel

The adhesive ability of the hydrogels to the host tissue was conducted by using fresh porcine skin according to our previous work [16]. The details are available in SI Materials and methods.

2.11. Antioxidant efficiency of hydrogels

The antioxidant efficiency of hydrogels was evaluated by the method of scavenging the stable 1, 1-diphenyl-2-picrylhydrazyl (DPPH) free radical [57]. The details are available in SI Materials and methods.

(a)

Samples	QCS (wt/vol)	PF127-CHO (wt/vol)	Gelation Time (37 °C)	-CHO/-NH_2
QCS/PF0.8	2%	14.4%	~90 s	0.8
QCS/PF1.0	2%	18.0%	~55 s	1.0
QCS/PF1.2	2%	21.6%	~30 s	1.2
QCS/PF1.3	2%	24.0%	<20 s	1.3
PF127-CHO	-	40.0%	~60-90 s	0

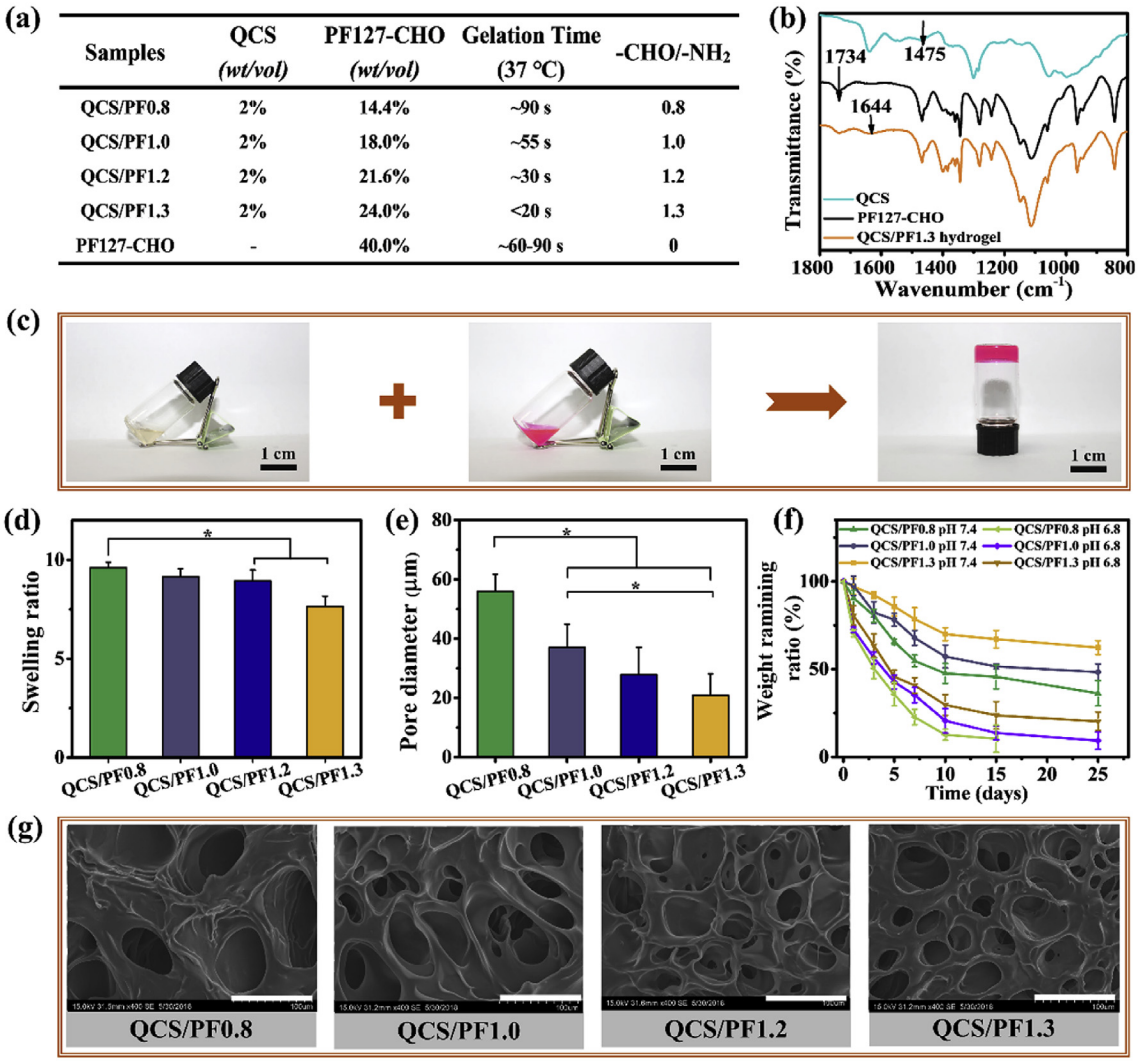

Fig. 2. Characterization of QCS/PF hydrogels. (a) Parameter and gelation time of hydrogel samples; (b) FT-IR spectra of QCS, PF127-CHO and QCS/PF hydrogel; (c) Photographs of QCS solution before crosslinking, PF127-CHO micelle solution (dyed with rhodamine B) and QCS/PF hydrogel. Scale bar: 1 cm; (d) Equilibrium swelling ratio of hydrogels after swelling for 24 h in PBS (pH 7.4) at 37 °C; (e) Pore size of hydrogels; (f) Degradation profiles of the hydrogels in PBS with pH 6.8 and 7.4 at 37 °C; (g) SEM images of hydrogels. Scale bar: 100 μm.

2.12. In vivo hemostatic ability test

Hemorrhaging liver mouse (Kunming mice, 30–35 g, female) were employed to evaluate the hemostatic potential of the QCS/PF1.0 hydrogels according to the reference [58,59]. The details are available in SI Materials and methods.

2.13. Cytocompatibility evaluation of the hydrogels

The cytocompatibility of QCS/PF hydrogels was determined by a direct contact method between hydrogels and mouse fibroblast (L929) cells. The details are available in SI Materials and methods.

2.14. Antibacterial activity evaluation

Escherichia coli (ATCC 8739) and *Staphylococcus aureus* (ATCC 29213) were employed to test the hydrogel surface antibacterial activity according to the reference [15,47]. The details are available in SI Materials and methods.

2.15. In vivo wound healing in a full-thickness skin defect model

The *in vivo* wound healing experiments were carried out by a full-thickness skin defect model according to our previous work [1], and Female Kunming mice (30–40 g, 5–6-week age) were employed in this study. The details are available in SI Materials and methods. All animal studies were approved by the animal research committee of Xi'an Jiaotong University.

2.16. Histologic analysis

The epidermal regeneration and inflammation in wound area were evaluated by using histopathologic examination. Subsequently, the sections were immunohistochemical stained with TNF-α and VEGF by using standard protocols. The details are available in SI Materials and methods.

2.17. Statistical analysis

Statistical differences (*$p < 0.05$) were determined using one-way ANOVA followed by Bonferroni post hoc test for multiple comparisons by SPSS, version 24 (IBM). In all cases, differences were considered

significant if $p < 0.05$. Results were expressed as mean ± standard deviation (SD).

3. Results and discussions

3.1. Synthesis of stretchable compressible self-healing injectable hydrogels

In this study, we designed a kind of self-healing injectable hydrogel dressing with excellent antibacterial property, good adhesiveness and blood clotting capacity. These hydrogels also exhibited good compressive and stretchable property and comparable modulus to human soft tissue [24]. The schematic representation of the hydrogel dressing was shown in Fig. 1. Although chitosan has abundant biomedical advantages, like benign gelation condition, antimicrobial ability, analgesic effect and hemostatic activity, the limited solubility in water and other organic solvents impedes its further applications [17,60,61]. In this work, quaternized chitosan (QCS) was chosen as the main material of the hydrogel due to its high solubility in physiological environment and enhanced antibacterial performance than chitosan [47,62]. The QCS polymer was firstly synthesized by grafting GTMAC on the chitosan chain (Fig. 1a). The QCS/PF hydrogels were synthesized by mixing QCS and PF127-CHO solution (Fig. 1b) together at physiological conditions (Fig. 1c), and amino groups from QCS and aldehyde groups from PF127-CHO polymer formed Schiff base bond in the hydrogel network. As a typical amphiphilic triblock copolymer, PF127 self-assembles into micelles in water (Fig. 1b), thus PF127 micelles act as dynamic micro-cross-linker in forming the first hydrogel network. Next, dynamic chemical bond (Schiff base) and the micelle cross-linking in one system formed this kind of hybrid physically–chemically cross-linked double network hydrogels (Fig. 1c), leading to the unique mechanical and self-healing property of QCS/PF hydrogel [39]. As shown in Fig. 1d, the original, bending, compression, stretching, twisting and knotting shapes of QCS/PF1.0 hydrogels exhibited their flexible mechanical properties. Four kinds of hydrogel samples were prepared by tuning the -CHO/-NH_2 ratio from 1.3 to 0.8, respectively. Fig. 2a shows detailed parameters and characterizations of QCS/PF hydrogel samples and 40% (*wt/vol*) of PF127-CHO hydrogel was chosen as a control group.

The chemical structures of QCS, PF127-CHO and QCS/PF hydrogel were confirmed by FT-IR in Fig. 2b. The obvious characteristic peak of 1475 cm^{-1} in QCS was assigned to the methyl bond of GTMAC [47,63], indicating that GTMAC was successfully grafted onto chitosan backbone. The peak at 1734 cm^{-1} in PF127-CHO was the stretching vibration of -C═O bond of aldehyde group, suggesting that -CHO was successfully introduced to PF127 [32]. A peak at 1644 cm^{-1} in QCS/PF hydrogel appeared due to the characteristic absorption of the newly formed Schiff base from amine group of QCS and aldehyde group of PF127-CHO [64], indicating that the hydrogel network was formed successfully. Furthermore, the weakened peak of 1734 cm^{-1} in the hydrogel also verified that -CHO in PF127-CHO polymer was partially consumed, and the results indicated that the QCS/PF hydrogels were successfully synthesized via dynamic Schiff base.

TGA is used to determine the thermal stability of the hydrogels, and the results are plotted in Fig. S2. The initial thermal decomposition of QCS polymer took place at 200 °C. The PF127-CHO began to decompose around 345 °C and the PF127-CHO was completely decomposed at 420 °C. The TGA curves of QCS/PF hydrogels showed a higher decomposition temperature at 370 °C, indicating that the hydrogels exhibited higher thermal stability than PF127-CHO. This is because hydrogels formed a condensed network by crosslinking between QCS and PF127-CHO.

3.2. Gelation time, swelling ratio, morphology and in vitro degradation of the hydrogels

The gelation time of hydrogels is important for biomedical application [65,66]. The method of recording the gelation time is tube inversion method (Fig. 2c) [67,68]. With the increase of concentration of PF127-CHO from 14.4% to 24% (*wt/vol)*, the gelation time of QCS/PF (Fig. 2a) decreased accordingly from 90 s to 20 s, because the hydrogel crosslinking density enhanced with more crosslinker addition. In addition, pure PF127-CHO hydrogel with high concentration (40%) was employed as a control. While its gelation time was longer than these series of self-healing stretchable hydrogels, due to its single crosslinking approach. Generally, these hydrogels with rapid gelation time are suitable for practical application. Usually, hydrogel dressing could maintain a considerable moist wound environment and could absorb tissue surplus exudates [1]. Herein, the equilibrated swelling ratios (ESR) of hydrogels were determined in PBS of pH = 7.4 at 37 °C after 24 h. In Fig. 2d, all the hydrogels could swell sharply (ESR > 8), but ESR of QCS/PF1.3 was lower than other three hydrogel groups which is attributed to its highest crosslinking density [68].

The morphologies of hydrogels were observed by SEM. All the hydrogels showed porous structures (Fig. 2g). The average diameter of QCS/PF1.3, QCS/PF1.2, QCS/PF1.0, and QCS/PF0.8 was 20 μm, 27 μm, 37 μm and 55 μm, respectively (Fig. 2e), and this is due to the increased crosslinking density in the hydrogel. The pore size of QCS/PF0.8 was larger than the other three groups ($p < 0.05$), and pore size of QCS/PF1.0 was larger than QCS/PF1.3 ($p < 0.05$). Hence, with the porous structure, the series of QCS/PF hydrogels have potential as wound dressing materials [7].

Considering the application in biomedical field [69], the degradation performance of the hydrogels was also evaluated. pH 7.4 PBS was chosen to simulate the physiological microenvironment. As shown in Fig. 2f, there were about 62% (QCS/PF1.3), 48% (QCS/PF1.0) and 36% (QCS/PF0.8) mass remaining after 25 days' incubation in PBS of pH 7.4, indicating that all these hydrogel groups exhibited desirable degradation characteristics for *in vivo* application.

3.3. Rheological properties and mechanical properties of QCS/PF hydrogels

Like ankle, knee, hip and wrist, these joints are movable and need to bend frequently. Hence, it's imperative that designing novel wound dressing materials with desirable mechanical properties, including stretchability, compression and recovery properties and mechanical stability. The Fig. 3a demonstrated good reversibility of QCS/PF1.0 hydrogel during elongation and relaxation. The tensile testing for these hydrogels was further carried out as shown in Fig. 3b, and the Young's modulus, tensile stress, and strain of the hydrogels were shown in Fig. 3c. The hydrogels showed suitable stretchability (76.1%–58.2%) for joint bending which matches the extensibility of the native skin (60–75%) perfectly [3], and QCS/PF1.3 with the highest PF127-CHO content exhibited the highest elongation-at-break (~76.1%). Ideally, the tensile moduli of hydrogel dressings should match the moduli of the underlying and neighboring tissues, because this could assure their integrity, and hydrogel adhesives can adhere to skin then secure wound safety until it is healed [23]. The Young's modulus of QCS/PF hydrogels was 21.5 kPa–37.3 kPa (Fig. 3c), which were comparable to human skin [24]. In addition, their moduli were similar to the modulus of a hybrid hydrogel with covalent and ionic crosslinking (~29 kPa) [35,70] and were higher than that of a hydrogen bonds based hydrogel (1.66 ± 0.47 kPa) [71].

The mechanical stability of hydrogels was evaluated using QCS/PF1.0 hydrogel sample by fifty successive loading – unloading cycles. In Fig. 3d, there were minor recovery losses existing in the latter cycles. After fifty successive loading – unloading cycles, a decrease of tensile stress (≈20%) of QCS/PF1.0 was recorded. And these demonstrated fatigue resistant property of the hydrogels [39]. The storage modulus (G′) and loss modulus (G″) of the hydrogels versus time were detected using a rheometer at fixed frequency (1 rad s^{-1}) to obtain the rheological properties of the hydrogels with different cross-linking densities. In Fig. 3e, with the increase of crosslinker concentration in the

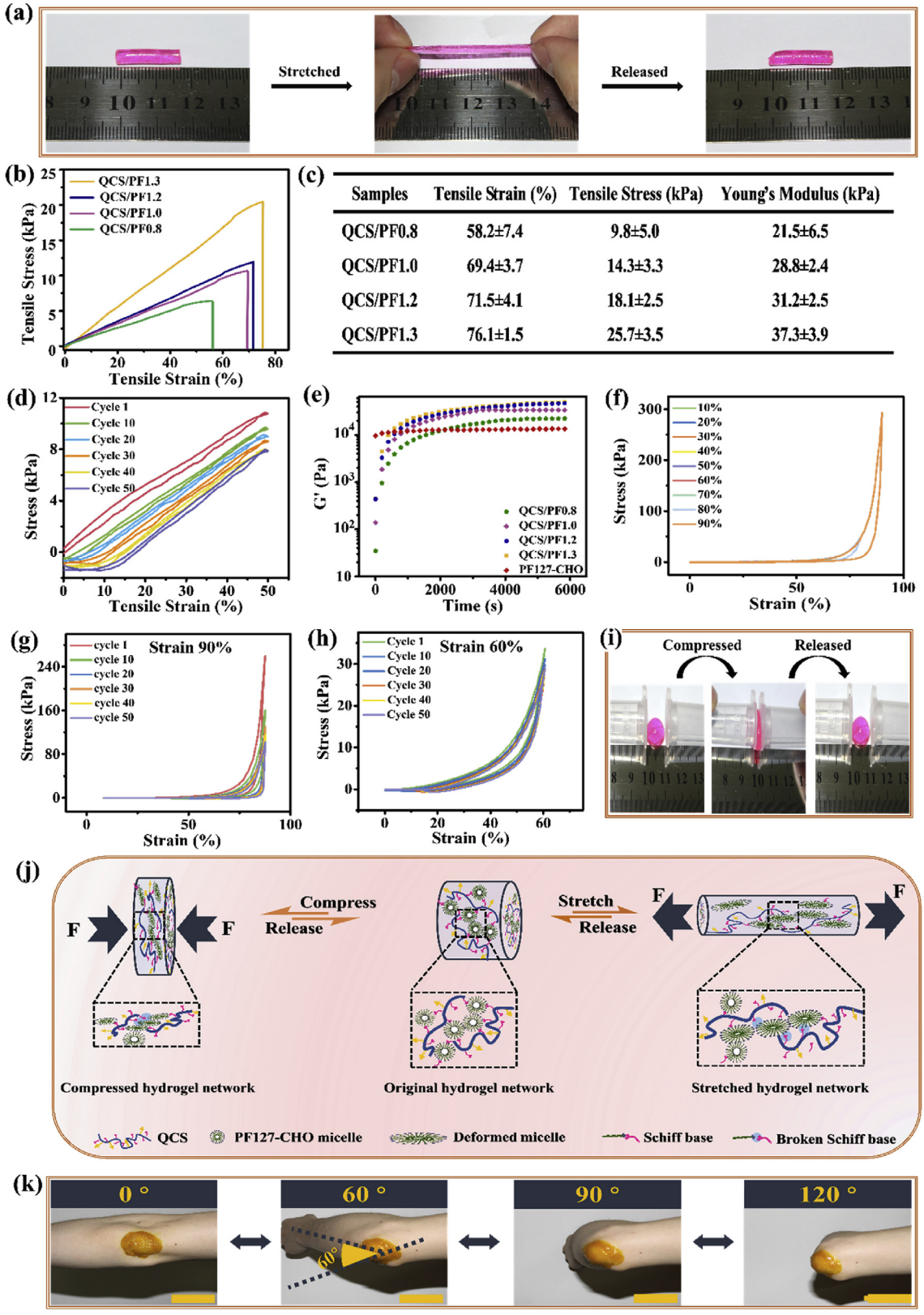

Samples	Tensile Strain (%)	Tensile Stress (kPa)	Young's Modulus (kPa)
QCS/PF0.8	58.2±7.4	9.8±5.0	21.5±6.5
QCS/PF1.0	69.4±3.7	14.3±3.3	28.8±2.4
QCS/PF1.2	71.5±4.1	18.1±2.5	31.2±2.5
QCS/PF1.3	76.1±1.5	25.7±3.5	37.3±3.9

Fig. 3. Mechanical characterizations of QCS/PF hydrogels. (a) Photographs of stretching and release process of QCS/PF1.0 hydrogel; (b) Stress−strain profile of hydrogels; (c) Summary of mechanical properties; (d) Cyclic tensile tests of QCS/PF1.0 hydrogel at a strain of 50% under the deformation rate of 30 mm/min; (e) Rheological behavior of hydrogels; (f) Compression and tension stress strain curves of QCS/PF1.0 hydrogel at strains from 10% to 90%; Compression and tension stress strain curves of QCS/PF1.0 hydrogel at strains of (g) 90% and (h) 60%; (i) Photographs of compression and release process of QCS/PF1.0 hydrogel; (j) The schematic diagram of the proposed mechanism for stretchable and compressive QCS/PF hydrogels; (k) Photograph of Cur-QCS/PF1.0 hydrogels that were applied on the human elbow. Scale bar: 5 cm.

hydrogels, the G′ of these hydrogels increased gradually from 22 kPa to 53 kPa. And all QCS/PF hydrogels exhibited higher G′ than our previous work and some single chemically crosslinked self-healing hydrogels which can provide stable crosslinking networks [1,16,26,29,32].

The compression and recovery properties were also comprehensively investigated [30]. In Fig. 3f, the QCS/PF1.0 hydrogels deformed and compressed when they were endured external compression at a set of strain from 10% to 90%, while they could recover to their initial shape quickly when the loading was released. When the hydrogels were subjected to 50 cyclic tensile tests with maximum compression strain of 90% (Fig. 3g), the hydrogels showed hysteresis and minor permanent deformations, suggesting energy dissipation existing in the hydrogel network [30,72]. At lower strain (60%) (Fig. 3h), neither serious plastic deformation nor strength decrease occurred in QCS/PF1.0 hydrogels, indicating their good robustness and resilience property. Additionally, these mechanical performances were superior to previous single physically/chemically crosslinked chitin-based hydrogel (fracture stress:40–50 kPa, fracture strain:27–50%) [73] and double-cross-linked chitin hydrogels (fracture strain: < 80%) [72]. Fig. 3i displayed good reversibility of QCS/PF1.0 hydrogel during compression and relaxation. All these results showed that QCS/PF hydrogels had stable and well-maintained network after 50 cycles loading.

As shown in Fig. 3j, this kind of hybrid micelle/hydrogel composite exhibited desirable mechanical properties which is attributed to the introduction of PF127 micelles and dynamic chemical Schiff base in the hydrogel. PF127 micelles acted as dynamic micro-cross-linkers in the hydrogel network, and they could break and dissipate energy upon loading, and reform during unloading, resulting in the recovery of hydrogels from deformation [35,39,74]. Besides this, chain sliding by the simultaneous fracture and reconfiguration of the Schiff base also caused the unique bonding feature [35]. Herein, combining the effect of dynamic Schiff base (covalent bonds) and micelle cross-linking interaction (non-covalent interactions) of PF127 in one system, endows the hydrogel stretchable, compressible and recovery mechanical properties [26,35]. Due to the good stretchability, compressive property and recovery, when the Cur-QCS/PF1.0 hydrogel was applied on the elbow (Fig. 3k), the experimenter could freely bend one's elbow (intersection angle from 0° to 180°) without any resistance, which verified the practical uses of this hydrogel as joint skin wound dressing.

3.4. Self-healing performance and injectability of QCS/PF hydrogels

Frequent motion and bending of joints could cause the traditional wound dressing's deformation, abrasion even damage when the dressing is bearing external mechanical force. Hence, self-healing hydrogels as new wound dressing could prolong their service time greatly. To evaluate the self-healing performance of the QCS/PF hydrogels, macroscopic self-healing test and rheological recovery test were performed. In Fig. 4a–f, the hydrogels were cut into disks with the same height (0.3 cm), and the hydrogel disks were then put together and placed at 25 °C for 2 h to make them heal without any external intervention. Then self-healed columnar hydrogel can be hold up under the force of gravity (Fig. 4f). Furthermore, the two different colors of hydrogel disks were cut into tiny pieces (Fig. 4b) and blended homogeneously (Fig. 4c). The mixture was put into a cylindrical mold for 2 h at room temperature. These hydrogel pieces could heal together and formed their original disk shape and there was no boundary among hydrogel pieces (Fig. 4d). Besides the excellent high self-healing efficacy, compared with single dynamic chemical bonds formed hydrogel, this chemically-physically linked hybrid hydrogel exhibited comparatively rapid self-healing rate. As shown in Fig. 4g and h, the rhodamine B dyed hydrogel (QCS/PF1.0) was cut into 2 pieces, and they could heal immediately within 3 s.

Rheological recovery test was further employed to evaluate the self-healing behavior of the hydrogels. From the results of strain amplitude sweep of the QCS/PF1.0 hydrogel (Fig. 4i), the intersection point between G′ and G″ was 113.7%, which means the collapse of the hydrogel network at this point. Afterwards, the continuous step strain method was used to perform the rheological recovery behavior of the hydrogel. Damage of the self-healing hydrogel after a higher strain and instant recovery of the hydrogel after healing at the lower strain were exhibited in Fig. 4j. At the high dynamic strain (200%), the G′ of the hydrogel decreased from 35000 Pa to 920 Pa, and G″ > G′, indicating the collapse of the hydrogel network. Due to the shear-thinning property of the hydrogels [75], they could be extruded through a 26-gauge needle without any clogging (Movie S1), indicating their good injectability. When the hydrogel was applied on low strain (1%), the G′ returned quickly to its initial value, indicating that the hydrogel network recovered efficiently. Furthermore, G′ and G″ of the original hydrogel and the hydrogel after experiencing cutting-healing process were measured (Fig. S3). The healed hydrogel showed nearly the same values of G′ and G″ with the original hydrogel, which indicated superior self-healing feature of QCS/PF hydrogel. The self-healing ability of the hydrogels is attributed to PF127 micelle physical cross-linking interaction, and the dynamic covalent Schiff-base bonds between the amine groups (QCS) and benzaldehyde (PF127-CHO).

Supplementary video related to this article can be found at https://doi.org/10.1016/j.biomaterials.2018.08.044.

3.5. In vitro antibacterial assay and in vitro cell compatibility for QCS/PF hydrogels

Besides acting as a barrier to protect the wound tissue from external bacterial infection, an optimum wound healing dressing possessing inherent antimicrobial properties would be more attractive [14]. In this study, the surface antibacterial activity of all QCS/PF hydrogels was evaluated using both *E. coli* (Gram-negative bacterium) and *S. aureus* (Gram-positive bacterium). In Fig. 5a–c, when contacting with bacterium for 2 h at 37 °C, all the hydrogel groups exhibited excellent killing ratio (> 90%) for both *S. aureus* and *E. coli*, indicating their excellent inherent antibacterial properties. Positive-charged amino groups and quaternary ammonium groups of QCS could damage the walls of the bacteria leading to the intracellular fluids release by electrostatic adherence with cytoderm of bacteria [47,57]. The Schiff bases including aromatic ring also played an important role on antimicrobial activity and Schiff base compounds have been proved to be promising leads for the design of more efficient antimicrobial agents [76]. Therefore, the combined action of active Schiff bases, protonated amino groups and quaternary ammonium groups endowed these hydrogels outstanding antibacterial performance. On the other hand, all the samples exhibited slightly lower activity against *E. coli* than *S. aureus*. This is because the structure of the cytoderm of *E. coli* is more complicated than that of the *S. aureus* [77]. Above all, all these hydrogels have good antibacterial properties.

The good cytocompatibility is the prerequisite for well-designed materials for biomedical field [78]. AlamarBlue® assay and LIVE/DEAD® Viability/Cytotoxicity Kit assay were used to evaluate QCS/PF hydrogels cytocompatibility. By using a direct contacting method, L929 cells were seeded in the 96-well plate with the same initial density and TCP was chosen as a control. In Fig. 5d, there was an obvious growth trend of cell proliferation among all the hydrogel groups during the three days. At the first day, compared with other hydrogel groups and TCP, QCS/PF1.3 hydrogel showed the lowest cell viability ($P < 0.05$). And, the other hydrogel formulations exhibited comparable cell viability with TCP. At the second day, all the groups showed pronounced L929 cells proliferation. After the L929 cells were continued to incubate from the second day to the third day, there was still continuous cell proliferation in all the groups. QCS/PF1.3 hydrogel exhibited lower cell number than QCS/PF1.0 and QCS/PF0.8 ($P < 0.05$), and there was a significant difference in cell viability among group of QCS/PF1.2, QCS/PF1.3 with TCP ($P < 0.05$). The QCS/PF1.0 exhibited good cytocompatibility with comparable cell number of TCP. For the LIVE/DEAD assay (Fig. 5e), the results agreed

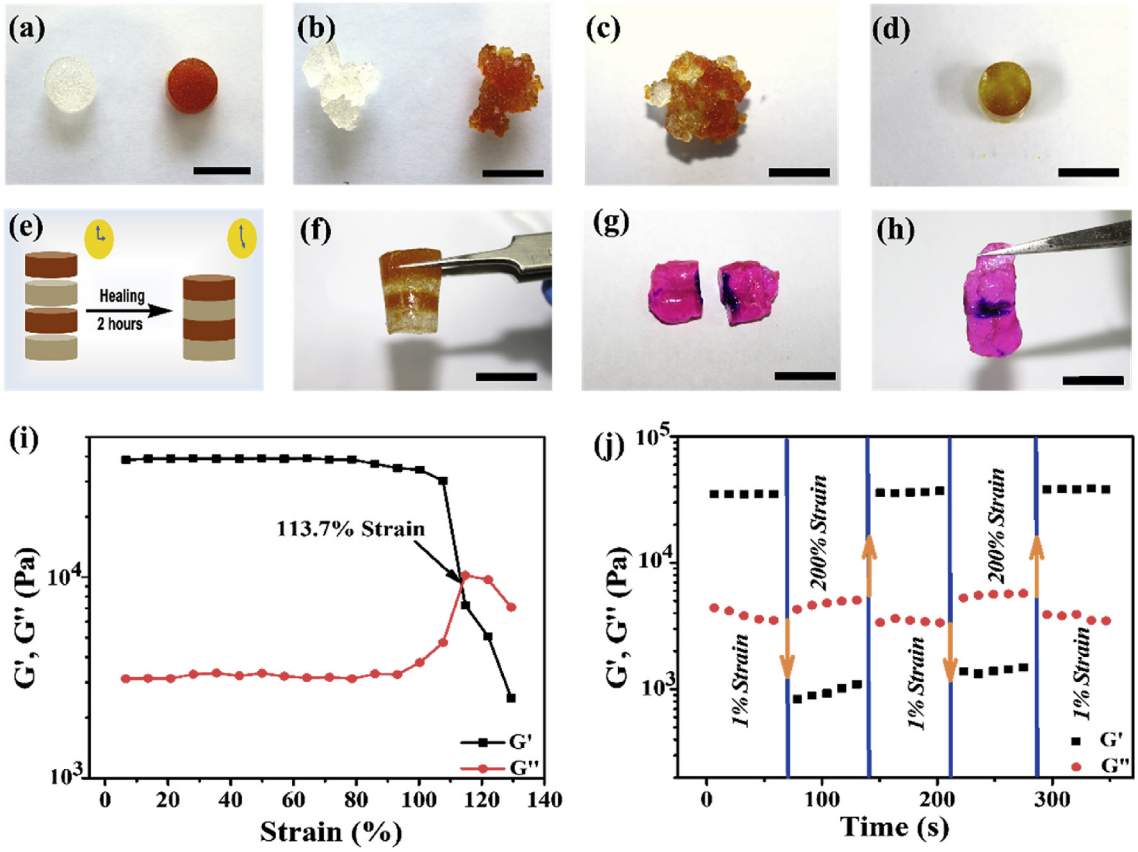

Fig. 4. Self-healing property of the hydrogels. (a) Two disk-shaped hydrogels (QCS/PF1.0 hydrogel and Cur-QCS/PF1.0 hydrogel); (b) The two different color hydrogel disks were cut into tiny pieces; (c) The hydrogel pieces were blended together and put into a cylindrical mold; (d) The hydrogel pieces healed completely into one block after 2 h at 25 °C; (e) Scheme of the self-healing process; (f) The hydrogel cylinders healed completely into one block after 2 h at 25 °C. (g–h) Photographs of hydrogels' rapid self-healing performance (< 3 s). Scale bar: 1 cm; (i) G′ and G″ on strain sweep and (j) the rheological properties of the hydrogel when alternate step strain switched from 1% to 200%. (For interpretation of the references to color in this figure legend, the reader is referred to the Web version of this article.)

with that of alamarBlue® assay. Majority of L929 cells, with a spindle-like morphology, were green in all the hydrogel groups and TCP after 3 days' incubation, and there were only few dead cells. All these results demonstrated that the QCS/PF1.0 hydrogels had good cytocompatibility as a promising candidate as wound dressing.

3.6. *In vitro* pH-responsive release behavior of Cur-QCS/PF hydrogels

Various studies have shown that the powerful modulating effects on wound healing of curcumin [18]. It has excellent biochemical effects, such as its anti-inflammatory, anti-infectious and anti-oxidant activity. And it has also been found that curcumin enhances the migration of fibroblast, collagen deposition and re-epithelization [14,18]. Hence, we employed curcumin as a model drug and encapsulated it in the hydrogel matrix to promote wound healing. Curcumin exhibited a turbid yellow suspension in water, indicating that curcumin could not be dissolved in aqueous solution (Fig. S4 (left)). Obviously, Cur-PF127-CHO mixture (Fig. S4 (right)) in water formed a transparent solution, demonstrating that PF127-CHO greatly promoted the solubility of curcumin in water due to the formation of PF127 micelles as shown in TEM image in Fig. 1c. The average micelle size of PF127, PF127-CHO and Cur-PF127-CHO were 120 nm, 115 nm and 179 nm, respectively (Fig. S5). The size of nanoparticles increased after the incorporation of curcumin into the micelles. The size of PF127-CHO by TEM observation (Fig. 1c) generally agreed with the result from DLS test. Furthermore, physiological milieu of the skin is acidic, which could support the natural barrier function and help to counteract microbial colonization [21]. Especially, majority of wounds, including acute wounds, wounds with pus or necrotic tissue and chronic wounds that progress in their healing process, show an acidic pH [79]. Therefore, it is desirable to develop new drug loaded wound dressing with the property of pH-responsiveness to meet patient's demand. The *in vitro* drug release behavior of these stretchable, self-healing hydrogels in different pH values (pH = 6.8, 6.0 and 7.4) of PBS as release medium was studied. In Fig. 6a and Fig. S6, compared with normal physiological environment (PBS, pH = 7.4), QCS/PF1.0 in acidic environment (PBS, pH = 6.8, 6.0) behaved faster release rate and more drug release amount in total. Specifically, in the earlier release stage (< 50 h), the group in the acidic environment showed higher release rate in terms of percentage (pH 6.0 > pH 6.8 > pH 7.4). After 288 h of incubation, approximately 78% of curcumin was released in PBS at pH 6.0, and about 61% and 28% curcumin were released in PBS at pH 6.8 and 7.4, respectively. These results indicated that these pH sensitive hydrogels released significantly more drug in the acid environment which was adapted to physiological skin milieu and majority of wounds. pH sensitive release property of the hydrogels was attributed to the pH-dependent degradation behavior of QCS/PF hydrogels [80]. As shown in Fig. 2f, all these hydrogel groups in the acidic PBS degraded quicker than that of physiological environment. This might be due to the protonation of the amino groups of chitosan at acidic pH, and thereafter the intramolecular electrostatic repulsion and enhanced hydrophilicity would make the hydrogel swell dramatically [32]. Furthermore, the cross-linking point Schiff base would be destroyed and decomposed gradually in acid medium [15]. Moreover, PF127-CHO content can also tune the release rate of curcumin (Fig. S7). Fig. 6g is the schematic diagram of application of the hydrogel dressing. When the hydrogel dressing is

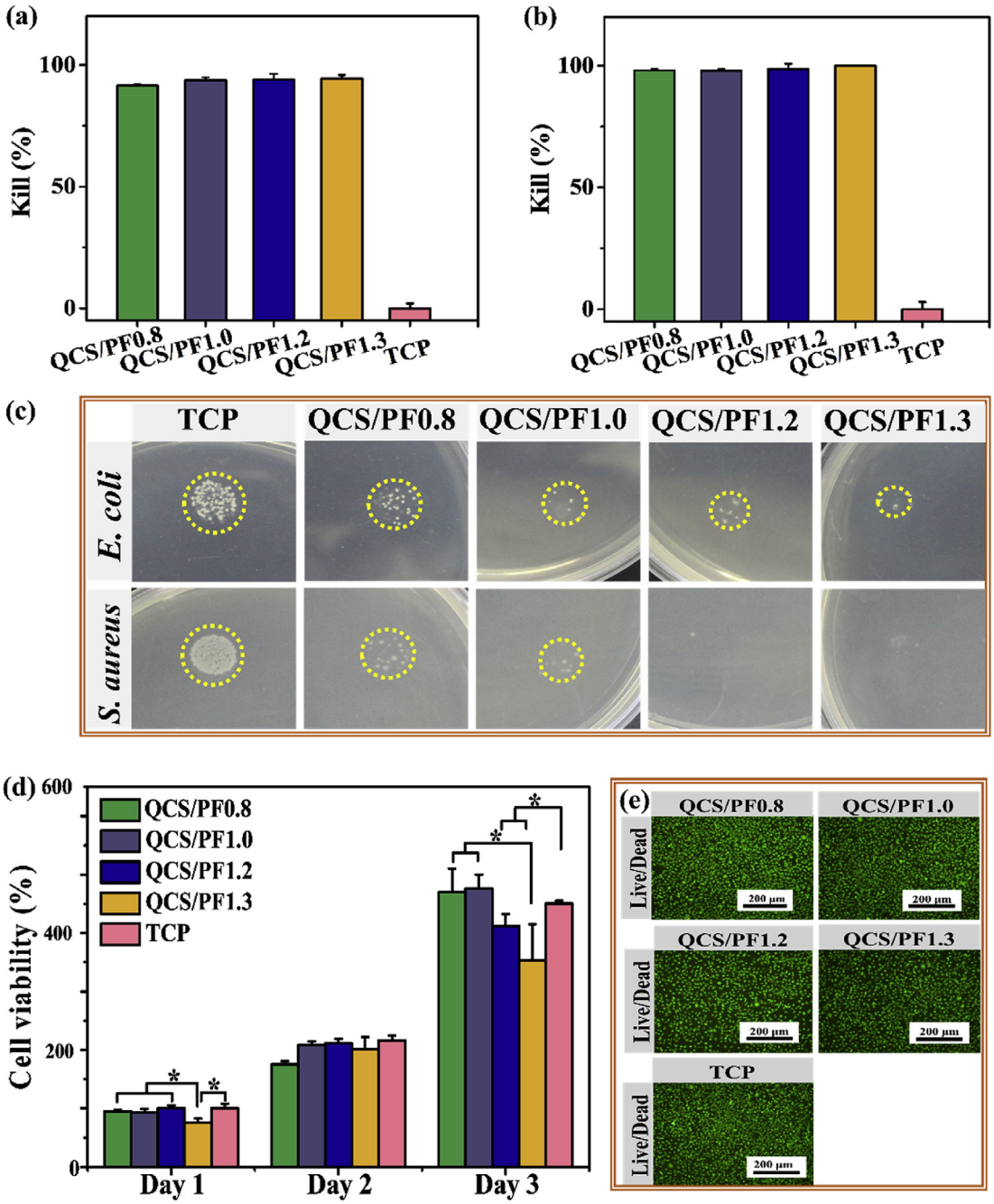

Fig. 5. Surface antibacterial activity against (a) *E. coli* and (b) *S. aureus* of QCS/PF hydrogels; Photographs of survival bacteria clones on agar plates after contacting with hydrogels: *E. coli* (c) and *S. aureus*; (d) Cell viability when contacting with hydrogels and TCP; (e) Live/dead staining of L929 cells after contacting with hydrogels and TCP for 3 days. Data indicate mean ± SD (n = 4). Error bar indicates standard deviation. *P < 0.05. Scale bar: 200 μm.

applied on the joints closely, the encapsulated drug (curcumin) can be released consistently.

3.7. Antioxidant ability of Cur-QCS/PF hydrogel

Enormous free radicals would exist in the wound site and these radicals will result in oxidative stress leading to lipid peroxidation, DNA breakage, and enzyme inactivation, including free radical scavenger enzymes etc. [14]. Curcumin has excellent antioxidant property to scavenge free radicals, improve significantly wound healing and protect tissues from oxidant [18]. Herein, the antioxidant activities of Cur-QCS/PF hydrogels and pure curcumin solution were evaluated by testing the scavenging efficiency for DPPH• [81]. Taken Cur-QCS/PF1.0 hydrogel as an example, there was obvious decrease in the intensity of DPPH• absorption peak after adding Cur-QCS/PF1.0 hydrogels (Fig. 6b and Fig. S8), indicating that these hydrogels had good antioxidant ability. Pure curcumin solution (Fig. S9) showed more obvious DPPH• scavenging efficiency at lower concentration (< 0.06 mg/mL). But hydrogel groups showed increased antioxidant ability with the increase of curcumin concentration (> 0.06 mg/mL, DPPH• scavenging efficiency > 80%). Overall, Cur-QCS/PF hydrogels with good antioxidant ability show great potential as wound dressing materials.

3.8. Adhesive property of QCS/PF hydrogels

Upon application, the hydrogel dressing must adhere to the wound

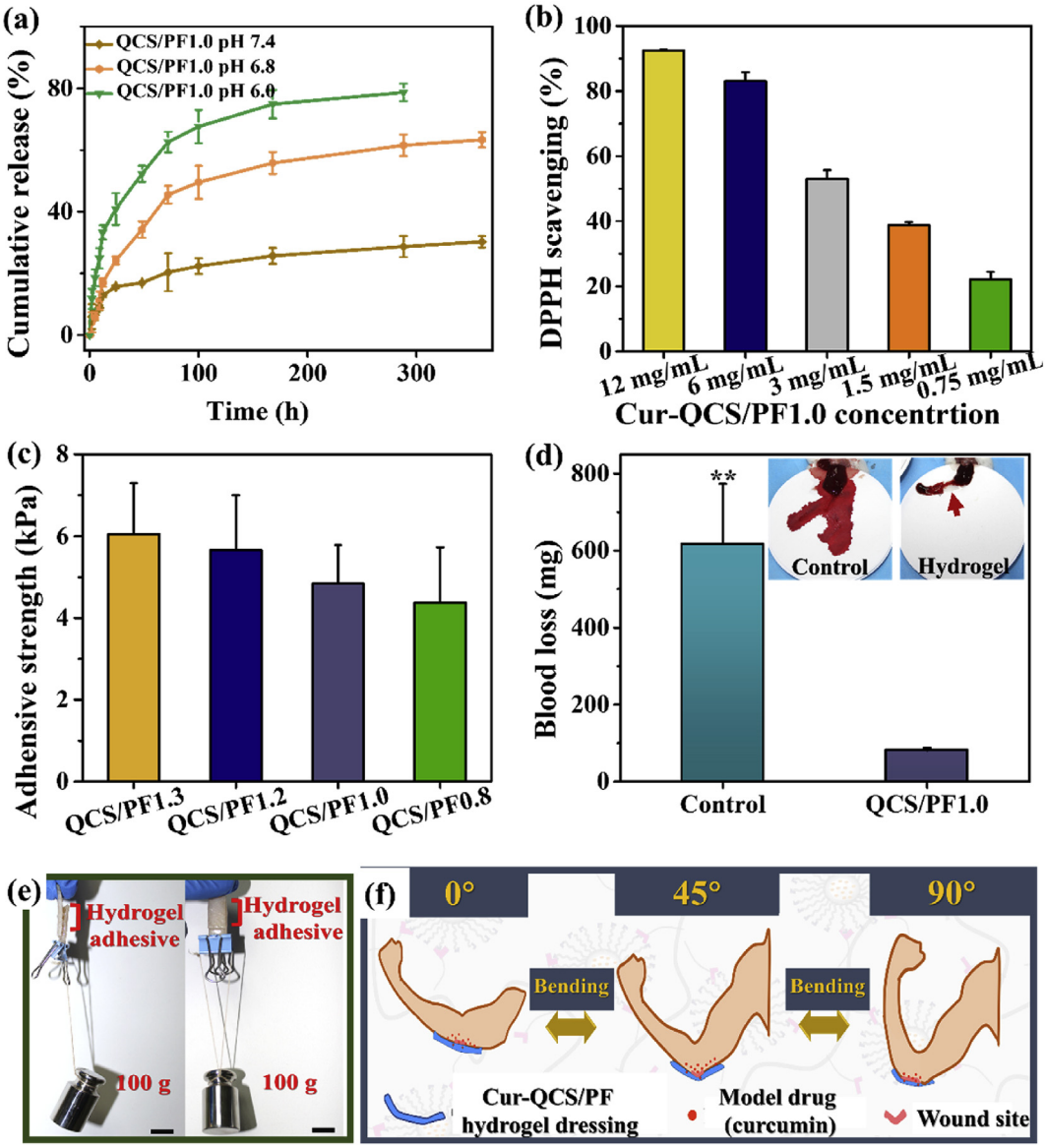

Fig. 6. (a) *In vitro* release kinetics of curcumin from the hydrogels in PBS at pH values of 7.4, 6.8 and 6.0; (b) DPPH scavenging percentage by Cur-QCS/PF1.0 hydrogels with different concentrations; (c) Adhesive strength of different hydrogels; (d) Hemostatic performance of hydrogel QCS/PF1.0; (e) Photographs of adhesive stress (weight = 100 g) of QCS/PF1.0 hydrogel on porcine skin. Scale bar: 1 cm; (f) Schematic diagram of model drug (curcumin) released from hydrogel when it was applied on the joints. **P < 0.01.

site completely and seal it to prevent bacterial cloning, as well as the exudation of fluids, by acting as an adhesive, hemostat, or sealant [23]. The adhesive strength of the hydrogels was evaluated employing a lap shear testing [16]. As shown in Fig. 6c, adhesive strength of the hydrogels increased gradually from 4.4 ± 1.3 kPa to 6.1 ± 1.2 kPa by increasing the content of PF127-CHO, and there was no significant difference among those groups. These series of hydrogels demonstrated desirable adhesive strength which was higher than our previous work [1,16] and maintained a comparable strength with fibrin glue adhesive (Greenplast®) (about 5 kPa) [59]. When applied on the porcine skin, the formed QCS/PF1.0 hydrogel adhesive could adhere the two pieces of porcine skin closely and withstand 100 g loads (Fig. 6c, e). This might be mainly because the Schiff base formation between aldehyde groups from PF127-CHO in the hydrogels and amine groups from surrounding tissue surface [1,23,82]. Moreover, chitosan could interact with the phospholipid molecules on the cell membranes via electrostatic and hydrophobic interactions which also contribute to the suitable adhesive strength of the hydrogels [83].

3.9. *In vivo* hemostatic performance and water vapor permeability for QCS/PF hydrogels

Hemostasis is the first phase of the natural process of wound healing which occurs upon injury [14]. Besides promoting platelet aggregation and thereby blood clot formation in the wound site, a suitable wound dressing could also adhere onto the surrounding tissue and solidify to serve as a bleeding-arrest quickly [84,85]. Hemostatic performance of QCS/PF1.0 hydrogel was evaluated by a hemorrhaging liver mouse model. In Fig. 6d, there was a significant difference of bleeding amount between these two groups (P < 0.01), and nearly 616.7 ± 157.0 mg blood was released from mouse' liver in the control group and only 80.1 ± 7.13 mg in the QCS/PF hydrogel group, which demonstrated the good *in vivo* hemostatic property of the hydrogels. QCS with positive charges has been a well-known hemostatic material [58]. Moreover, with the short gelation time (~55 s), stable gelation network (G′ = ~33700 Pa) and high adhesive properties, QCS/PF1.0 hydrogels could provide a synergistic effect on the hemostatic property.

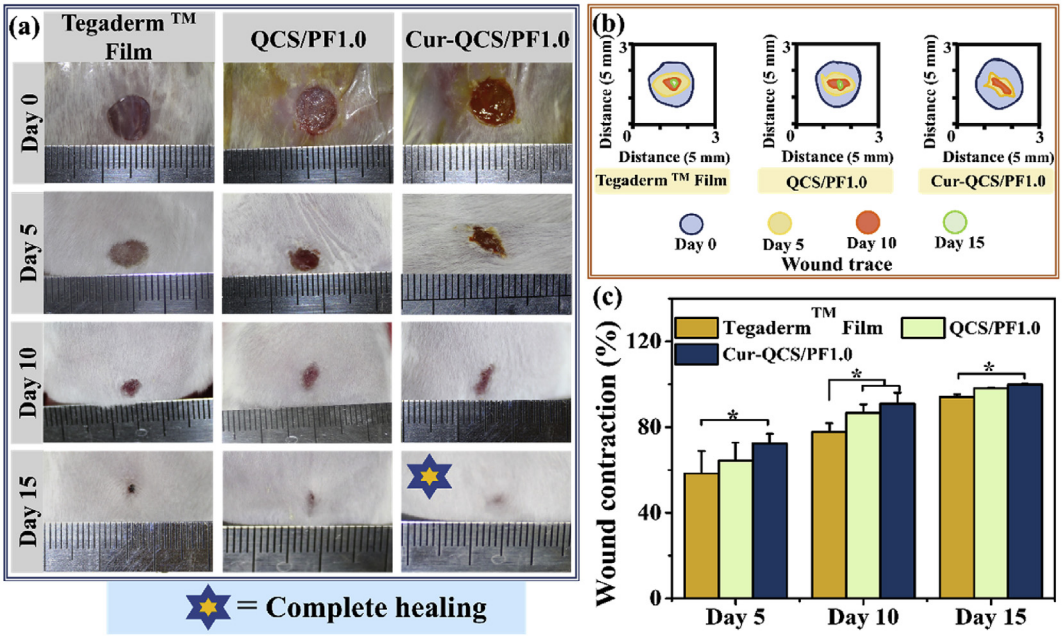

Fig. 7. (a) Photographs of wounds at 0^{th}, 5th, 10th and 15th day for commercial film dressing (Tegaderm™) (control), QCS/PF1.0 hydrogel and Cur-QCS/PF1.0 hydrogel; (b) Traces of wound-bed closure during 15 days for each treatment; (c) Wound contraction for each treatment. *P < 0.05.

Furthermore, permeability is important for wound dressing and the water vapor permeability of QCS/PF1.0 hydrogel was assessed by the amount of water evaporated from a container sealed using the hydrogel films. As shown in the Fig. S10, compared with Tegaderm™ film, the QCS/PF1.0 hydrogel groups displayed a higher water vapor permeability (P < 0.05), indicating the good permeability of the hydrogels.

3.10. In vivo wound healing

The wound healing effect of hydrogel wound dressing is further evaluated in a full-thickness skin defect model. In Fig. 7a–c, the wound contraction of Cur-QCS/PF1.0, QCS/PF1.0 and commercial films (control group) groups were displayed on 0^{th} day, 5th day, 10th day and 15th day, respectively. On the 5th day, all the groups showed wound area reduction to some extent, while Cur-QCS/PF1.0 hydrogel exhibited the largest wound contraction area (72%, P < 0.05) which demonstrated its comparatively higher promotion effect on wound healing. On the 10th day, both two hydrogel groups exhibited better therapeutic effect than control group. The wound contraction area of QCS/PF1.0 group exceeded nearly 9% (P < 0.05) than commercial films and Cur-QCS/PF1.0 group was 13% higher (P < 0.05) than commercial films. On 15th day, although all the groups exhibited extremely tiny wound remaining area, Cur-QCS/PF1.0 hydrogel group still had about 5% lead than commercial film dressing group in wound contraction. Therefore, the results from QCS/PF1.0 hydrogels demonstrated their better wound healing effect than control group by tracing the wound contraction area, which was attributed to the combined effects of the inherent antibacterial performance of QCS [86], hemostatic performance, chitosan's desirable function in promotion of wound healing [87], and moist wound environment provided by hydrogel dressing [88]. When the hydrogel dressing was encapsulated with bioactive drug (curcumin), the Cur-QCS/PF1.0 showed the best therapeutic effect during overall wound healing stages. This is because curcumin could expedite the different wound healing stages (inflammation, proliferation, and remodeling), as it can scavenge ROS effectively, increase the production of anti-oxidant enzymes around wound environment during the inflammation phrase [18]. It also promotes fibroblast migration, the formation of granulation tissue and collagen, and re-epithelialization in the proliferation phrase. And curcumin also plays an important role on remodeling phrase, where it improves wound contraction by increasing the number of cytokines to enhance fibroblasts proliferation [18,89,90]. Overall, the hydrogel QCS/PF1.0 exhibited slightly better therapeutic effect on wound healing than commercial film dressing, and Cur-QCS/PF1.0 hydrogels showed much better effect on the whole process of wound healing.

3.11. Histological analysis

Wound healing is a specific biological process which is comprised of following overlapping but well-defined phases: hemostasis, inflammation, migration, proliferation and remodeling [7]. Hematoxylin and eosin stained sections (H&E staining) were employed to evaluate the wound healing progress in different phases. As shown in Fig. 8a, all the groups showed mild acute inflammatory responses on the fifth day, and there were numbers of inflammatory cells and fibroblasts migrating to the wound site. While, compared with commercial film (control) and QCS/PF1.0 hydrogel group, Cur-QCS/PF1.0 hydrogels exhibited relatively more fibroblast cells and less inflammatory cells around the wound site, which is attributed to the well anti-inflammation and anti-oxidant action of curcumin [14]. And this phenomenon corresponds to the migration phase of healing process that Cur-QCS/PF1.0 hydrogels promoted a quicker healing process among all the compared groups. On the tenth day, all the hydrogel groups formed a layer of epithelium. Compared with other groups, hydrogel Cur-QCS/PF1.0 group showed higher regularity of both epithelium and connective tissue with more fibroblasts. Furthermore, hydrogel groups (Cur-QCS/PF1.0, QCS.PF1.0) exhibited more blood vessels and hair follicles than control group. When it comes to the 15th day, besides the formation of basic structure of epithelium and dermis in control group, a few blood vessels and hair follicles were formed in the QCS/PF1.0 hydrogel group. Particularly, the maximum amount mature blood vessels, hair follicles, thickened epidermis and well-proliferated fibroblast demonstrated the best wound healing effect of Cur-QCS/PF1.0 among the three groups.

Some growth factors and abundant fibroblasts consist of the granulation tissue together [91]. Hence, a thicker granulation tissue is an important indicator to evaluate the wound healing process [54]. As shown in Fig. 8b and c, after 15 days' application, the granulation tissue in commercial film exhibited nearly 550 μm thinner than Cur-QCS/

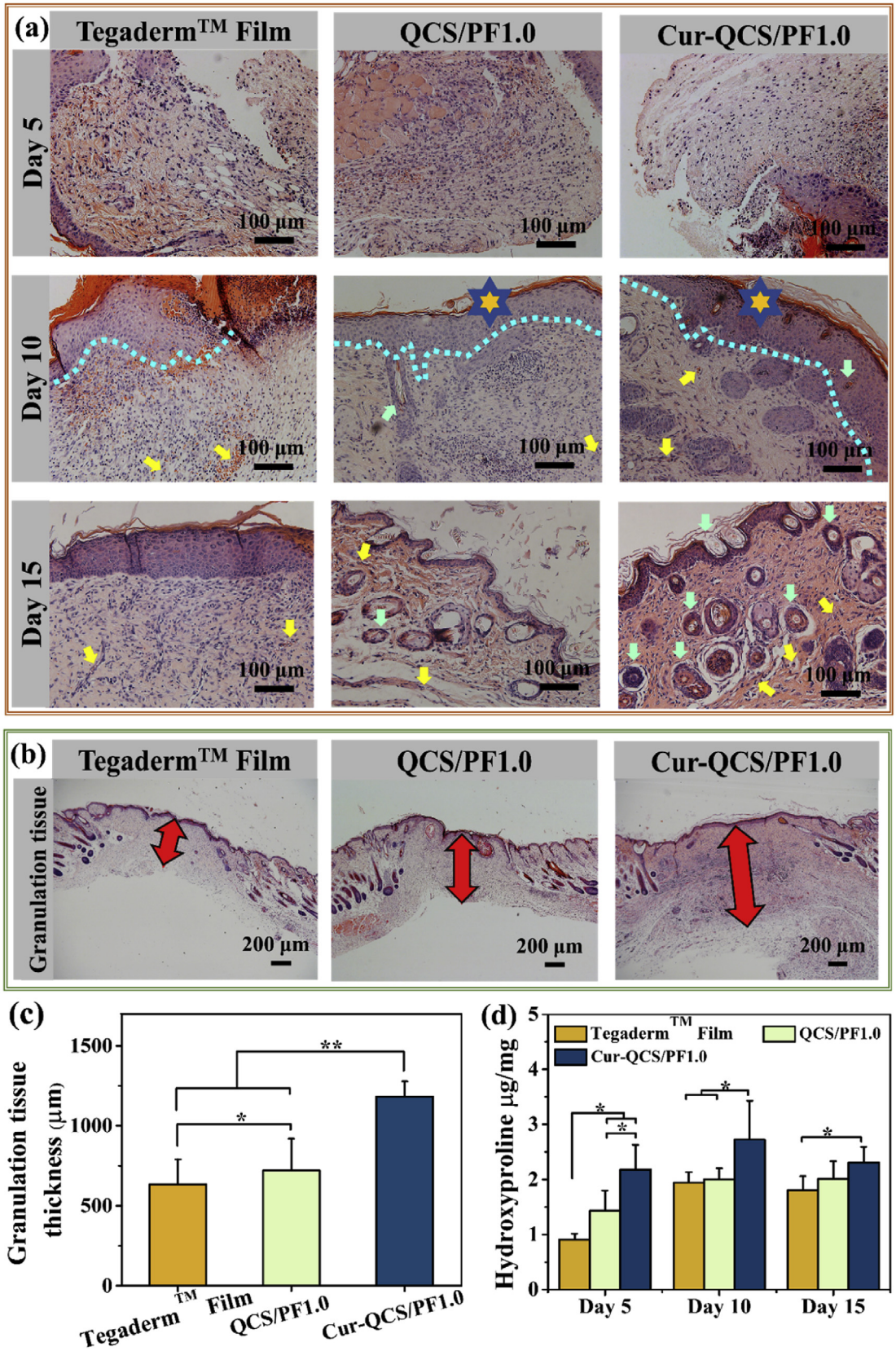

Fig. 8. (a) Histomorphological evaluation of wound regeneration for commercial film dressing (Tegaderm™), QCS/PF1.0 hydrogel and Cur-QCS/PF1.0 hydrogel on 5th, 10th, and 15th day (blood vessels: yellow arrows, hair follicles: green arrows, boundary of epithelium and dermis: blue lines, completed epithelium: yellow hexagram). Scale bar: 100 μm. (b) Granulation tissue thickness for commercial film dressing (Tegaderm™), QCS/PF1.0 hydrogel and Cur-QCS/PF1.0 hydrogel on 15th day (granulation tissue: red arrows). Scale bar: 200 μm. (c) Statistical graph of granulation tissue thickness for different treatments on 15th day. (d) Collagen amount in commercial film dressing (Tegaderm™), hydrogel QCS/PF1.0 and Cur-QCS/PF1.0 hydrogel by determining the hydroxyproline. *P < 0.05, **P < 0.01. (For interpretation of the references to color in this figure legend, the reader is referred to the Web version of this article.)

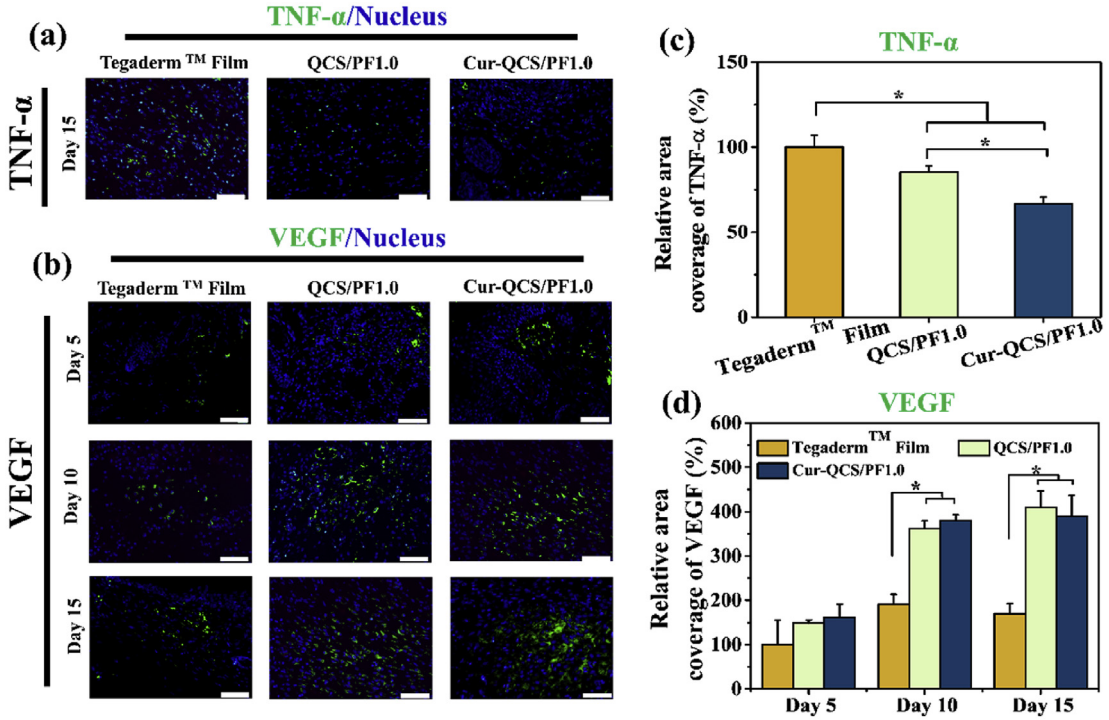

Fig. 9. Representative photographs of skin wound tissues on day 5, day 10 and day 15 after immunofluorescence labeling with (a) TNF-α (green) and (b) VEGF (green). Scale bar: 60 μm. Quantified analysis of the relative percentage of area coverage by TNF-α-actinin (c) and VEGF (d), respectively. For all data, the control group was set as 100%. *P < 0.05. (For interpretation of the references to color in this figure legend, the reader is referred to the Web version of this article.)

PF1.0 hydrogel group (P < 0.01) and nearly 220 μm thinner than QCS/PF1.0 hydrogel group (P < 0.05). Therefore, by promoting thickness of granulation tissue, the QCS/PF1.0 hydrogel demonstrated the better wound healing effect than control, and the curcumin loaded group (Cur-QCS/PF1.0 hydrogel) demonstrated the extraordinary therapeutic effect in these three groups.

In summary, the migration of inflammatory cells and high density of fibroblast (5th day), the formation of complete structure of epithelium (10th day), more numbers of mutual blood vessels and hair follicles, high density of fibroblasts, and thicker thickness of granulation tissue (15th day) suggested that Cur-QCS/PF1.0 group shows the prominent wound healing effect, and hydrogel group (QCS/PF1.0) exhibited a better treatment effect than control group.

3.12. Collagen deposition analysis of wound regeneration

Considering the migration of fibroblasts to the wound area, the total collagen level in granulation tissue was tested to evaluate the therapeutic effects among three treatments by analyzing the hydroxyproline content. As shown in Fig. 8d, the content of collagen in all groups kept rising during the first 10 days, and on the fifteenth day, they maintained at a stable level. Compared with control group, QCS/PF1.0 and Cur-QCS/PF1.0 hydrogel groups exhibited superior collagen level during the 15 days. Furthermore, when the QCS/PF1.0 hydrogel was loaded with curcumin, the Cur-QCS/PF1.0 showed more prominent collagen level than the other groups (P < 0.05) throughout the whole test period. Hence, all the hydrogel groups showed better treatment effect than commercial films, and the drug loaded hydrogel group (Cur-QCS/PF1.0) demonstrated the best healing effect during the experimental groups.

3.13. TNF-α and VEGF expression in wound regeneration with different treatments

Infections could cause severe inflammatory response to postpone the process of wound healing. As a kind of typical proinflammatory factor, tumor necrosis factor-α (TNF-α), was chosen to evaluate the efficacy of the hydrogel dressing in preventing infection [51]. In Fig. 9 (a) and (c), the expression of TNF-α in control commercial film group was higher than the two hydrogel groups on the 15th day (*P < 0.05), which suggested more severe inflammatory responses in control group. This is because QCS is an efficient inherent antibacterial material to reduce infection. Especially, Cur-QCS/PF1.0 exhibited the least expression of TNF-α (*P < 0.05), because curcumin could reduce production of TNF-α [9a]. Vascular endothelial growth factor (VEGF) regulates multiple pathways during wound healing including angiogenesis, re-epithelization and collagen synthesis [1a]. During the regeneration period, all the therapeutic groups expressed VEGF (Fig. 9 (b) and (d)). While, there was higher expression level in the hydrogel groups than control (*P < 0.05). By simultaneously reducing production of proinflammatory factor (TNF-α) and upregulating the expression of VEGF, hydrogel groups promoted the wound healing process effectively. Overall, these results suggested that QCS/PF1.0 and Cur-QCS/PF1.0 hydrogels significantly accelerated wound closure and a better treatment effect than control group.

4. Conclusions

A series of injectable hydrogel wound dressings with multi-functions including inherent antibacterial property, self-healing, stretchable and compressive property act as a novel joint skin wound healing dressing were developed, and their excellent therapeutic effects on wound healing were demonstrated by a full-thickness skin defect model in terms of wound healing rate, granulation tissue thickness and collagen disposition. The QCS/PF hydrogels were successfully synthesized based on QCS and PF127-CHO polymer under physiological conditions. These hydrogels exhibited stable rheological property, similar modulus to human soft tissue, tunable gelation time, excellent adhesion property, good pH-dependent degradation ability, biocompatibility, higher drug released rate in acidic skin environment behavior, inherent

antibacterial property and free radical scavenging capacity which could effectively enhance the wound healing process. Moreover, QCS/PF1.0 hydrogel showed good *in vivo* blood clotting capacity as hydrogel wound dressing. Furthermore, the hydrogels showed faster wound healing rate with balanced inflammatory infiltration, greater granulation tissue thickness, higher density of fibroblasts and collagen deposition in a full-thickness skin defect model than commercial dressing (Tegaderm™). Especially, by upregulating wound healing process related factors (VEGF) and reducing production of proinflammatory factor (TNF-α), curcumin incorporated QCS/PF1.0 hydrogel presented the best wound healing effect among all groups. All these results demonstrated that QCS/PF1.0 hydrogel with multi-functions could greatly promote the wound healing process, and their moderate stretchability, compressibility, excellent self-healing ability and pH-responsive ability is compelling as wound dressing material in joints skin wound healing.

Acknowledgement

This work was supported by the National Natural Science Foundation of China (grant number: 51673155]), State Key Laboratory for Mechanical Behavior of Materials (grant number: 20182002) and “the Fundamental Research Funds for the Central Universities”. We also thank Dr. Wang at Instrument Analysis Center of Xi'an Jiaotong University for their assistance with DLS analysis.

Appendix A. Supplementary data

Supplementary data related to this article can be found at https://doi.org/10.1016/j.biomaterials.2018.08.044.

References

[1] X. Zhao, H. Wu, B. Guo, R. Dong, Y. Qiu, P.X. Ma, Antibacterial anti-oxidant electroactive injectable hydrogel as self-healing wound dressing with hemostasis and adhesiveness for cutaneous wound healing, Biomaterials 122 (2017) 34–47.
[2] R. Xu, G.X. Luo, H.S. Xia, W.F. He, J. Zhao, B. Liu, J.L. Tan, J.Y. Zhou, D.S. Liu, Y.Z. Wang, Z.H. Yao, R.X. Zhan, S.S. Yang, J. Wu, Novel bilayer wound dressing composed of silicone rubber with particular micropores enhanced wound re-epithelialization and contraction, Biomaterials 40 (2015) 1–11.
[3] N. Annabi, D. Rana, E. Shirzaei Sani, R. Portillo-Lara, J.L. Gifford, M.M. Fares, S.M. Mithieux, A.S. Weiss, Engineering a sprayable and elastic hydrogel adhesive with antimicrobial properties for wound healing, Biomaterials 139 (2017) 229–243.
[4] B. Guo, P.X. Ma, Conducting polymers for tissue engineering, Biomacromolecules 19 (2018) 1764–1782.
[5] C. Gong, Q. Wu, Y. Wang, D. Zhang, F. Luo, X. Zhao, Y. Wei, Z. Qian, A biodegradable hydrogel system containing curcumin encapsulated in micelles for cutaneous wound healing, Biomaterials 34 (2013) 6377–6387.
[6] B. Guo, L. Glavas, A.-C. Albertsson, Biodegradable and electrically conducting polymers for biomedical applications, Prog. Polym. Sci. 38 (2013) 1263–1286.
[7] Z. Fan, B. Liu, J. Wang, S. Zhang, Q. Lin, P. Gong, L. Ma, S. Yang, A novel wound dressing based on Ag/graphene polymer hydrogel: effectively kill bacteria and accelerate wound healing, Adv. Funct. Mater. 24 (2014) 3933–3943.
[8] N.Q. Tran, Y.K. Joung, E. Lih, K.D. Park, In situ forming and rutin-releasing chitosan hydrogels as injectable dressings for dermal wound healing, Biomacromolecules 12 (2011) 2872–2880.
[9] J. Boateng, O. Catanzano, Advanced therapeutic dressings for effective wound healing-A review, J. Pharmacol. Sci. 104 (2015) 3653–3680.
[10] D.R. Griffin, W.M. Weaver, P.O. Scumpia, D. Di Carlo, T. Segura, Accelerated wound healing by injectable microporous gel scaffolds assembled from annealed building blocks, Nat. Mater. 14 (2015) 737–744.
[11] J. Hoque, B. Bhattacharjee, R.G. Prakash, K. Paramanandham, J. Haldar, Dual function injectable hydrogel for controlled release of antibiotic and local antibacterial therapy, Biomacromolecules 19 (2017) 267–278.
[12] M. Yadollahi, H. Namazi, M. Aghazadeh, Antibacterial carboxymethyl cellulose/Ag nanocomposite hydrogels cross-linked with layered double hydroxides, Int. J. Biol. Macromol. 79 (2015) 269–277.
[13] P.T.S. Kumar, V.K. Lakshmanan, T.V. Anilkumar, C. Ramya, P. Reshmi, A.G. Unnikrishnan, S.V. Nair, R. Jayakumar, Flexible and microporous chitosan hydrogel/nano ZnO composite bandages for wound dressing: in vitro and in vivo evaluation, ACS Appl. Mater. Interfaces 4 (2012) 2618–2629.
[14] D. Gopinath, M.R. Ahmed, K. Gomathi, K. Chitra, P.K. Sehgal, R. Jayakumar, Dermal wound healing processes with curcumin incorporated collagen films, Biomaterials 25 (2004) 1911–1917.
[15] J. Qu, X. Zhao, P.X. Ma, B. Guo, Injectable antibacterial conductive hydrogels with dual response to an electric field and ph for localized “smart” drug release, Acta Biomater. 72 (2018) 55–69.
[16] R. Dong, X. Zhao, B. Guo, P.X. Ma, Self-healing conductive injectable hydrogels with antibacterial activity as cell delivery Carrier for cardiac cell therapy, ACS Appl. Mater. Interfaces 8 (2016) 17138–17150.
[17] M. Yadollahi, I. Gholamali, H. Namazi, M. Aghazadeh, Synthesis and characterization of antibacterial carboxymethylcellulose/CuO bio-nanocomposite hydrogels, Int. J. Biol. Macromol. 73 (2015) 109–114.
[18] D. Akbik, M. Ghadiri, W. Chrzanowski, R. Rohanizadeh, Curcumin as a wound healing agent, Life Sci. 116 (2014) 1–7.
[19] M. Kulac, C. Aktas, F. Tulubas, R. Uygur, M. Kanter, M. Erboga, M. Ceber, B. Topcu, O.A. Ozen, The effects of topical treatment with curcumin on burn wound healing in rats, J. Mol. Histol. 44 (2013) 83–90.
[20] R.K. Maheshwari, A.K. Singh, J. Gaddipati, R.C. Srimal, Multiple biological activities of curcumin: a short review, Life Sci. 78 (2006) 2081–2087.
[21] L.A. Schneider, A. Korber, S. Grabbe, J. Dissemond, Influence of pH on wound-healing: a new Perspective for wound-therapy? Arch. Dermatol. Res. 298 (2007) 413–420.
[22] I. Castangia, A. Nacher, C. Caddeo, D. Valenti, A.M. Fadda, O. Diez-Sales, A. Ruiz-Sauri, M. Manconi, Fabrication of quercetin and curcumin bionanovesicles for the prevention and rapid regeneration of full-thickness skin defects on mice, Acta Biomater. 10 (2014) 1292–1300.
[23] C. Ghobril, M.W. Grinstaff, The chemistry and engineering of polymeric hydrogel adhesives for wound closure: a tutorial, Chem. Soc. Rev. 44 (2015) 1820–1835.
[24] X. Chen, Making electrodes stretchable, Small Methods 1 (2017) 1600029.
[25] M. Amjadi, S. Sheykhansari, B.J. Nelson, M. Sitti, Recent advances in wearable transdermal delivery systems, Adv. Mater. 30 (2018) 1704530.
[26] Z. Wei, J.H. Yang, J. Zhou, F. Xu, M. Zrinyi, P.H. Dussault, Y. Osada, Y.M. Chen, Self-healing gels based on constitutional dynamic chemistry and their potential applications, Chem. Soc. Rev. 43 (2014) 8114–8131.
[27] X. Yan, Z. Liu, Q. Zhang, J. Lopez, H. Wang, H.C. Wu, S. Niu, H. Yan, S. Wang, T. Lei, J. Li, D. Qi, P. Huang, J. Huang, Y. Zhang, Y. Wang, G. Li, J.B. Tok, X. Chen, Z. Bao, Quadruple h-bonding cross-linked supramolecular polymeric materials as substrates for stretchable, antitearing, and self-healable thin film electrodes, J. Am. Chem. Soc. 140 (2018) 5280–5289.
[28] Z. Wei, J.H. Yang, Z.Q. Liu, F. Xu, J.X. Zhou, M. Zrínyi, Y. Osada, Y.M. Chen, Novel biocompatible polysaccharide-based self-healing hydrogel, Adv. Funct. Mater. 25 (2015) 1352–1359.
[29] T.C. Tseng, L. Tao, F.Y. Hsieh, Y. Wei, I.M. Chiu, S.H. Hsu, An injectable, self-healing hydrogel to repair the central nervous system, Adv. Mater. 27 (2015) 3518–3524.
[30] Z. Deng, Y. Guo, X. Zhao, P.X. Ma, B. Guo, Multifunctional stimuli-responsive hydrogels with self-healing, high conductivity, and rapid recovery through host–guest interactions, Chem. Mater. 30 (2018) 1729–1742.
[31] Y.B. Wu, L. Wang, X. Zhao, S. Hou, B.L. Guo, P.X. Ma, Self-healing supramolecular bioelastomers with shape memory property as a multifunctional platform for biomedical applications via modular assembly, Biomaterials 104 (2016) 18–31.
[32] J. Qu, X. Zhao, P.X. Ma, B. Guo, pH-responsive self-healing injectable hydrogel based on n-carboxyethyl chitosan for hepatocellular carcinoma therapy, Acta Biomater. 58 (2017) 168–180.
[33] H. Yu, Y. Liu, H. Yang, K. Peng, X. Zhang, An injectable self-healing hydrogel based on chain-extended PEO-PPO-PEO multiblock copolymer, Macromol. Rapid Commun. 37 (2016) 1723–1728.
[34] B. Yan, J. Huang, L. Han, L. Gong, L. Li, J.N. Israelachvili, H. Zeng, Duplicating dynamic strain-stiffening behavior and nanomechanics of biological tissues in a synthetic self-healing flexible network hydrogel, ACS Nano 11 (2017) 11074–11081.
[35] P. Wang, G. Deng, L. Zhou, Z. Li, Y. Chen, Ultrastretchable, self-healable hydrogels based on dynamic covalent bonding and triblock copolymer micellization, ACS Macro Lett. 6 (2017) 881–886.
[36] B.L. Guo, P.X. Ma, Synthetic biodegradable functional polymers for tissue engineering: a brief review, Sci. China Chem. 57 (2014) 490–500.
[37] D.C. Tuncaboylu, M. Sari, W. Oppermann, O. Okay, Tough and self-healing hydrogels formed via hydrophobic interactions, Macromolecules 44 (2011) 4997–5005.
[38] Y.N. Sun, G.R. Gao, G.L. Du, Y.J. Cheng, J. Fu, Super tough, ultrastretchable, and thermoresponsive hydrogels with functionalized triblock copolymer micelles as macro-cross-linkers, ACS Macro Lett. 3 (2014) 496–500.
[39] Q. Chen, L. Zhu, H. Chen, H. Yan, L. Huang, J. Yang, J. Zheng, A novel design strategy for fully physically linked double network hydrogels with tough, fatigue resistant, and self-healing properties, Adv. Funct. Mater. 25 (2015) 1598–1607.
[40] M.S. Akash, K. Rehman, Recent progress in biomedical applications of pluronic (PF127): pharmaceutical perspectives, J. Contr. Release 209 (2015) 120–138.
[41] J.S. Choi, H.S. Yoo, Pluronic/chitosan hydrogels containing epidermal growth factor with wound-adhesive and photo-crosslinkable properties, J. Biomed. Mater. Res. 95 (2010) 564–573.
[42] S.P. Quah, A.J. Smith, A.N. Preston, S.T. Laughlin, S.R. Bhatia, Large-area alginate/PEO-PPO-PEO hydrogels with thermoreversible rheology at physiological temperatures, Polymer 135 (2018) 171–177.
[43] S. Farhoudian, M. Yadollahi, H. Namazi, Facile synthesis of antibacterial chitosan/CuO bio-nanocomposite hydrogel beads, Int. J. Biol. Macromol. 82 (2016) 837–843.
[44] S. Javanbakht, N. Nazari, R. Rakhshaei, H. Namazi, Cu-crosslinked carboxymethylcellulose/naproxen/graphene quantum dot nanocomposite hydrogel beads for naproxen oral delivery, Carbohydr. Polym. 195 (2018) 453–459.
[45] Y. Ren, X. Zhao, X. Liang, P.X. Ma, B. Guo, Injectable hydrogel based on quaternized chitosan, gelatin and dopamine as localized drug delivery system to treat Parkinson's disease, Int. J. Biol. Macromol. 105 (2017) 1079–1087.
[46] H. Namazi, R. Rakhshaei, H. Hamishehkar, H.S. Kafil, Antibiotic loaded

carboxymethylcellulose/MCM-41 nanocomposite hydrogel films as potential wound dressing, Int. J. Biol. Macromol. 85 (2016) 327–334.
[47] X. Zhao, P. Li, B. Guo, P.X. Ma, Antibacterial and conductive injectable hydrogels based on quaternized chitosan-graft-polyaniline/oxidized dextran for tissue engineering, Acta Biomater. 26 (2015) 236–248.
[48] C. Gong, S. Deng, Q. Wu, M. Xiang, X. Wei, L. Li, X. Gao, B. Wang, L. Sun, Y. Chen, Y. Li, L. Liu, Z. Qian, Y. Wei, Improving antiangiogenesis and anti-tumor activity of curcumin by biodegradable polymeric micelles, Biomaterials 34 (2013) 1413–1432.
[49] L. Li, J. Ge, B. Guo, P.X. Ma, In situ forming biodegradable electroactive hydrogels, Polym. Chem. 5 (2014) 2880.
[50] R. Rakhshaei, H. Namazi, A potential bioactive wound dressing based on carboxymethyl cellulose/ZnO impregnated MCM-41 nanocomposite hydrogel, Mater. Sci. Eng. C Mater. Biol. Appl. 73 (2017) 456–464.
[51] S. Barkhordari, M. Yadollahi, H. Namazi, pH sensitive nanocomposite hydrogel beads based on carboxymethyl cellulose/layered double hydroxide as drug delivery systems, J. Polym. Res. 21 (2014).
[52] S. Javanbakht, H. Namazi, Doxorubicin loaded carboxymethyl cellulose/graphene quantum dot nanocomposite hydrogel films as a potential anticancer drug delivery system, Mater. Sci. Eng. C Mater. Biol. Appl. 87 (2018) 50–59.
[53] J. Zhao, B. Guo, P.X. Ma, Injectable alginate microsphere/PLGA–PEG–PLGA composite hydrogels for sustained drug release, RSC Adv. 4 (2014) 17736.
[54] Y. Dong, S. A, M. Rodrigues, X. Li, S.H. Kwon, N. Kosaric, S. Khong, Y. Gao, W. Wang, G.C. Gurtner, Injectable and tunable gelatin hydrogels enhance stem cell retention and improve cutaneous wound healing, Adv. Funct. Mater. 27 (2017) 1606619.
[55] X. Zhao, R. Dong, B. Guo, P.X. Ma, Dopamine-incorporated dual bioactive electroactive shape memory polyurethane elastomers with physiological shape recovery temperature, high stretchability, and enhanced C2C12 myogenic differentiation, ACS Appl. Mater. Interfaces 9 (2017) 29595–29611.
[56] L. Wang, Y. Wu, B.L. Guo, P.X. Ma, Nanofiber yarn/hydrogel core-shell scaffolds mimicking native skeletal muscle tissue for guiding 3D myoblast alignment, elongation, and differentiation, ACS Nano 9 (2015) 9179-9179.
[57] R. Gharibi, H. Yeganeh, A. Rezapour-Lactoee, Z.M. Hassan, Stimulation of wound healing by electroactive, antibacterial, and antioxidant polyurethane/siloxane dressing membranes: in vitro and in vivo evaluations, ACS Appl. Mater. Interfaces 7 (2015) 24296–24311.
[58] J.H. Ryu, Y. Lee, W.H. Kong, T.G. Kim, T.G. Park, H. Lee, Catechol-functionalized chitosan/pluronic hydrogels for tissue adhesives and hemostatic materials, Biomacromolecules 12 (2011) 2653–2659.
[59] E. Lih, J.S. Lee, K.M. Park, K.D. Park, Rapidly curable chitosan-PEG hydrogels as tissue adhesives for hemostasis and wound healing, Acta Biomater. 8 (2012) 3261–3269.
[60] B.L. Guo, J.F. Yuan, Q.Y. Gao, Preparation and release behavior of temperature- and pH-responsive chitosan material, Polym. Int. 57 (2008) 463–468.
[61] X. Zhao, B. Guo, H. Wu, Y. Liang, P.X. Ma, Injectable antibacterial conductive nanocomposite cryogels with rapid shape recovery for noncompressible hemorrhage and wound healing, Nat. Commun. 9 (2018) 2784.
[62] Z.X. Peng, L. Wang, L. Du, S.R. Guo, X.Q. Wang, T.T. Tang, Adjustment of the antibacterial activity and biocompatibility of hydroxypropyltrimethyl ammonium chloride chitosan by varying the degree of substitution of quaternary ammonium, Carbohydr. Polym. 81 (2010) 275–283.
[63] J. Cho, J. Grant, M. Piquette-Miller, C. Allen, Synthesis and physicochemical and dynamic mechanical properties of a water-soluble chitosan derivative as a biomaterial, Biomacromolecules 7 (2006) 2845–2855.
[64] B.L. Guo, A. Finne-Wistrand, A.C. Albertsson, Facile synthesis of degradable and electrically conductive polysaccharide hydrogels, Biomacromolecules 12 (2011) 2601–2609.
[65] Y. Wu, B. Guo, P.X. Ma, Injectable electroactive hydrogels formed via host–guest interactions, ACS Macro Lett. 3 (2014) 1145–1150.
[66] Y. Wu, L. Wang, B. Guo, P.X. Ma, Interwoven aligned conductive nanofiber yarn/hydrogel composite scaffolds for engineered 3D cardiac anisotropy, ACS Nano 11 (2017) 5646–5659.
[67] L. Li, M. Yu, P.X. Ma, B. Guo, Electroactive degradable copolymers enhancing osteogenic differentiation from bone marrow derived mesenchymal stem cells, J. Mater. Chem. B 4 (2016) 471–481.
[68] L. Li, J. Ge, P.X. Ma, B. Guo, Injectable conducting interpenetrating polymer network hydrogels from gelatin-graft-polyaniline and oxidized dextran with enhanced mechanical properties, RSC Adv. 5 (2015) 92490–92498.
[69] B. Guo, A. Finne-Wistrand, A.-C. Albertsson, Degradable and electroactive hydrogels with tunable electrical conductivity and swelling behavior, Chem. Mater. 23 (2011) 1254–1262.
[70] J.Y. Sun, X.H. Zhao, W.R.K. Illeperuma, O. Chaudhuri, K.H. Oh, D.J. Mooney, J.J. Vlassak, Z.G. Suo, Highly stretchable and tough hydrogels, Nature 489 (2012) 133–136.
[71] I. Jeon, J.X. Cui, W.R.K. Illeperuma, J. Aizenberg, J.J. Vlassak, Extremely stretchable and fast self-healing hydrogels, Adv. Mater. 28 (2016) 4678–4683.
[72] Y.Q. Liu, K.G. Xu, Q. Chang, M.A. Darabi, B.J. Lin, W. Zhong, M. Xing, Highly flexible and resilient elastin hybrid cryogels with shape memory, injectability, conductivity, and magnetic responsive properties, Adv. Mater. 28 (2016) 7758–7767.
[73] D. Xu, J. Huang, D. Zhao, B. Ding, L. Zhang, J. Cai, High-flexibility, high-toughness double-cross-linked chitin hydrogels by sequential chemical and physical cross-linkings, Adv. Funct. Mater. 28 (2016) 5844–5849.
[74] U. Gulyuz, O. Okay, Self-healing poly(acrylic acid) hydrogels with shape memory behavior of high mechanical strength, Macromolecules 47 (2014) 6889–6899.
[75] S. Hou, X.F. Wang, S. Park, X.B. Jin, P.X. Ma, Rapid self-integrating, injectable hydrogel for tissue complex regeneration, Adv. Healthc. Mater. 4 (2015) 1491–1495.
[76] M.S.M. Eldin, E.A. Soliman, A.I. Hashem, T.M. Tamer, Antimicrobial activity of novel aminated chitosan derivatives for biomedical applications, Adv. Polym. Technol. 31 (2012) 414–428.
[77] C.Q. Qin, Q. Xiao, H.R. Li, M. Fang, Y. Liu, X.Y. Chen, Q. Li, Calorimetric studies of the action of chitosan-N-2-hydroxypropyl trimethyl ammonium chloride on the growth of microorganisms, Int. J. Biol. Macromol. 34 (2004) 121–126.
[78] Y. Wu, L. Wang, B. Guo, Y. Shao, P.X. Ma, Electroactive biodegradable polyurethane significantly enhanced schwann cells myelin gene expression and neurotrophin secretion for peripheral nerve tissue engineering, Biomaterials 87 (2016) 18–31.
[79] S. Schreml, R.M. Szeimies, S. Karrer, J. Heinlin, M. Landthaler, P. Babilas, The impact of the pH value on skin integrity and cutaneous wound healing, J. Eur. Acad. Dermatol. 24 (2010) 373–378.
[80] B.L. Guo, J.F. Yuan, Q.Y. Gao, pH and ionic sensitive chitosan/carboxymethyl chitosan IPN complex films for the controlled release of coenzyme A, Colloid Polym. Sci. 286 (2007) 175–181.
[81] P.A. Kilmartin, M. Gizdavic-Nikolaldis, Z. Zujovic, J. Travas-Sejdic, G.A. Bowmaker, R.P. Cooney, Free radical scavenging and antioxidant properties of conducting polymers examined using EPR and NMR spectroscopies, Synth. Met. 153 (2005) 153–156.
[82] Y. Murakami, M. Yokoyama, T. Okano, H. Nishida, Y. Tomizawa, M. Endo, H. Kurosawa, A novel synthetic tissue-adhesive hydrogel using a crosslinkable polymeric micelle, J. Biomed. Mater. Res. 80 (2007) 421–427.
[83] F.J. Pavinatto, A. Pavinatto, L. Caseli, D.S. dos Santos, T.M. Nobre, M.E.D. Zaniquelli, O.N. Oliveira, Interaction of chitosan with cell membrane models at the air-water interface, Biomacromolecules 8 (2007) 1633–1640.
[84] S. Enoch, J.E. Grey, K.G. Harding, ABC of wound healing-recent advances and emerging treatments, BMJ Br. Med. J. 332 (2006) 962–965.
[85] A.J. Singer, R.A.F. Clark, Mechanisms of disease-cutaneous wound healing, N. Engl. J. Med. 341 (1999) 738–746.
[86] Z.Z. Zhou, D. Yan, X.J. Cheng, M. Kong, Y. Liu, C. Feng, X.G. Chen, Biomaterials based on N,N,N-trimethyl chitosan fibers in wound dressing applications, Int. J. Biol. Macromol. 89 (2016) 471–476.
[87] H. Ueno, T. Mori, T. Fujinaga, Topical formulations and wound healing applications of chitosan, Adv. Drug Deliv. Rev. 52 (2001) 105–115.
[88] J.S. Xiao, S.Y. Chen, J. Yi, H.F. Zhang, G.A. Ameer, A cooperative copper metal-organic framework-hydrogel system improves wound healing in diabetes, Adv. Funct. Mater. 27 (2017).
[89] A. Bajaj, M.R.P. Rao, A. Pardeshi, D. Sali, Nanocrystallization by evaporative antisolvent technique for solubility and bioavailability enhancement of telmisartan, Aaps, Pharmscitech 13 (2012) 1331–1340.
[90] A. Asai, T. Miyazawa, Occurrence of orally administered curcuminoid as glucuronide and glucuronide/sulfate conjugates in rat plasma, Life Sci. 67 (2000) 2785–2793.
[91] P. Mostafalu, G. Kiaee, G. Giatsidis, A. Khalilpour, M. Nabavinia, M.R. Dokmeci, S. Sonkusale, D.P. Orgill, A. Tamayol, A. Khademhosseini, A textile dressing for temporal and dosage controlled drug delivery, Adv. Funct. Mater. 27 (2017) 1702399.